BNWL-1756
Special
Distribution

kB

THE MTR-PHOENIX FUEL EXPERIMENT: BURNUP ANALYSES AND CORRELATIONS

Battelle
Pacific Northwest Laboratories
Richland, Washington 99352

JUNE 1973

Prepared for the U.S. Atomic Energy
Commission under Contract AT(45-1):1830

BNWL-1756

NOTICE

This report was prepared as an account of work sponsored by the United States Government. Neither the United States nor the United States Atomic Energy Commission, nor any of their employees, makes any warranty, express or implied, or assumes any legal liability or responsibility for the accuracy, completeness or usefulness of any information, apparatus, product, or process disclosed, or represents that its use would not infringe privately-owned rights.

PACIFIC NORTHWEST LABORATORY
operated by
BATTELLE
for the
U.S. ATOMIC ENERGY COMMISSION
Under Contract AT(45-1)-1830

Printed in the United States of America
Available from
National Technical Information Service
U.S. Department of Commerce
5285 Port Royal Road
Springfield, Virginia 22151
Price: Printed Copy $3.00; Microfiche $0.95

AEC RL RICHLAND, WASH

BNWL-1756
Special Distribution

3 3679 00062 2912

THE MTR-PHOENIX FUEL EXPERIMENT: BURNUP ANALYSES AND CORRELATIONS

Edited By

R. I. Smith

With Contributions From

D. A. Kottwitz

D. R. Oden

U. P. Jenquin

NUCLEAR ENGINEERING DEPARTMENT

June 1973

BATTELLE
PACIFIC NORTHWEST LABORATORIES
Richland, Washington 99352

ABSTRACT

A burnup experiment was performed in the MTR at NRTS which utilized a full core loading of Phoenix fuel (Aℓ-21 wt% Pu with 23 at% ^{240}Pu). Results from this experiment included the variation of isotopic composition with burnup and with position throughout the core and the measured rates of reactivity loss with burnup. The measured results are compared with the results of calculations made for Phoenix fuel core in MTR. Conclusions are drawn concerning the adequacy of the computational methods and calculational models used in the comparisons.

TABLE OF CONTENTS

		Page No.
	LIST OF FIGURES	i
	LIST OF TABLES	ii
I.	INTRODUCTION	1
II.	SUMMARY	2
III.	THE MTR PHOENIX FUEL BURNUP EXPERIMENT	3
	A. Core Description	3
	B. Operating History During the Burnup Experiment	9
	C. Burnup Monitoring	12
	1. Flux Wands	12
	2. Fuel Plates	14
	3. Measured Fission Product Data	21
IV.	THEORY-EXPERIMENT COMPARISONS	24
	A. Calculational Models and Methods	24
	1. Description of Computational Models	25
	B. Comparisons of Measured and Calculated Isotopic Concentrations	27
	1. Measured Isotopic Data	27
	2. Ratios of Effective Cross Sections	31
	3. Least Squares Analysis of Isotopic Data	32
	C. Reactivity Loss Rate Comparisons	38
	1. Measured Reactivity Loss Rates	38
	2. Calculated Reactivity Loss Rates	41
V.	CONCLUSIONS	45
VI.	REFERENCES	46
VII.	APPENDICES	
	A. Analytical Results from Phoenix Fuel Wand Samples	48
	B. Analytical Results from Phoenix Fuel Plate Samples	51

LIST OF FIGURES

		Page No.
1.	MTR Lattice Loadings for Standard and Phoenix Cores . . .	4
2.	MTR-Phoenix Fuel Element and Plate	6
3.	MTR-Phoenix Fuel Element with Flux Monitoring Position and Flux Monitor	7
4.	MTR-Phoenix Core Power History	10
5.	Rods-Out k_{eff} vs. MTR-Phoenix Core Burnup	11
6.	Phoenix Fuel Experiment-MTR Core Loading	13
7.	Axial Burnup Profiles from Flux Monitor Wands	15
8.	Horizontal Burnup Profile from Fuel Plates	18
9.	Axial Burnup Profile from Fuel Plates	19
10.	Typical Gamma Ray Spectrum from a Flux Wand	22
11.	Comparison of the Ratios of Pu Isotopic Concentration at Beginning of Life to End of Life as a Function of Burnup of Total Initial Pu, Measured and Calculated	29
12.	Excess Reactivity versus Burnup for MTR Cores	40
13.	Variation of MTR-Phoenix Core Reactivity, Measured and Calculated	43

LIST OF TABLES

		Page No.
I.	Isotopic Composition of Plutonium in Phoenix Fuel	8
II.	Flux Wand History in MTR-Phoenix Core	12
III.	Summary of Destructive Analysis of Flux Wand Samples	16
IV.	Summary of Destructive Analysis of Fuel Plate Samples	20
V.	Relative Net Photopeak Areas Measured using a GeLi Detector System	23
VI.	Atom Densities for Cell Calculations	26
VII.	Results of Least Squares Fits of Wand Data.	36
VIII.	Results of Least Squares Fits of Fuel Plate Data	37
IX.	Comparison of MTR-Phoenix Fuel Core with Previous MTR Cores .	39
X.	Burnup Parameters of MTR Cores	42

THE MTR-PHOENIX FUEL EXPERIMENT: BURNUP ANALYSES AND CORRELATIONS

I. INTRODUCTION

A burnup experiment has been completed in the Materials Testing Reactor (MTR) at the National Reactor Testing Station (NRTS) in Idaho utilizing a full core of Aluminum-21 wt% plutonium alloy fuel. This experiment was the culmination of an extensive research and development program into the use of plutonium which contained large (>20%) fractions of the ^{240}Pu isotope as a fuel for small, high power reactors, conducted for the USAEC's Division of Reactor Development and Technology by Battelle-Northwest. Fuel of this type has been called Phoenix Fuel based on the concept of converting the fertile absorber ^{240}Pu into fissile ^{241}Pu, thus enhancing the reactivity lifetime of the core without increasing the initial core reactivity.

The MTR-Phoenix Fuel Experiment was accomplished in three phases. Phase I consisted of an extensive critical experiment program in a mock-up of the MTR, performed in the Plutonium Recycle Critical Facility[1]. Correlation of these experiments together with earlier critical studies[2,3] have been reported by Heeb[4].

Phase II consisted of a comprehensive program of zero power measurements performed during the loading of the Phoenix core in MTR and at outages throughout the burn-down of the core[5].

The final phase, which consisted of the post-irradiation examinations, non-destructive and destructive analyses, and correlation of these results with calculation, is the subject of this report.

II. SUMMARY

The burnup experiment in the MTR using Phoenix fuel demonstrated the basic premise of the Phoenix concept, that ^{240}Pu could be utilized as a convertible poison in a reactor to obtain a longer reactivity lifetime without increasing the initial core reactivity. While a similar lifetime result can be obtained using 20% enriched uranium, the plutonium core has the advantage of producing a higher thermal flux in the reflector per watt of reactor power. Thus, in a test reactor such as MTR whose purpose is to provide a high thermal neutron flux at sample positions in the reflector, the plutonium core provides the same flux levels at a lower reactor power level.

A significant body of data has been obtained relating to the variation of plutonium isotopic compositions with burnup and with location in core, as well as measured rates of reactivity loss with burnup. These data are unique since the plutonium isotope burnup and transmutations are unobscured by production of fresh ^{239}Pu from ^{238}U captures. The MTR-Phoenix Experiment is the only full core burnup experiment using only plutonium fuel that has been carefully sampled for analysis.

The correlations performed have demonstrated that a core of the MTR type is an extremely complex computational problem. The variation in the neutron energy spectrum with position throughout the core is an important factor, one which requires a high degree of spatial detail in the calculation. Nevertheless, the body of data obtained from the MTR-Phoenix Fuel Experiment provides a valuable basis for further examination and improvement in methods, models, and cross sections.

III. THE MTR-PHOENIX FUEL BURNUP EXPERIMENT

A full-core burnup experiment is an expensive, time-consuming undertaking. However, it is the only effective way to evaluate the adequacy of methods and/or data being used in reactor calculations. The performance of the experiment in MTR has been reported previously[5]. Details of the core design and the power performance are repeated here to provide understanding of the experimental results and to facilitate an understanding of the computational problems associated with the burnup experiment analysis.

A. Core Description

The Materials Testing Reactor[6,7] is a rather heterogeneous assembly, with a plate-type core of aluminum alloy fuel that is moderated and cooled with light water, and reflected with beryllium, graphite and light water. The core measured approximately 9 inches north to south by 28 inches east to west by 24 inches high. Surrounding the core was a beryllium reflector which was 39 3/8 inches high and extended out to a diameter of 54 inches. Beyond this was a graphite reflector zone, which measured 12 feet north to south by about 15 feet east to west by 9 feet 4 inches high. The bottom of the graphite was located 4 feet below the core horizontal centerline.

The Phoenix Fuel core consisted of 19 fuel elements and 8 fuel-follower shim-safety rods located in the central 3 rows of the 5 x 9 lattice in the MTR, as shown in Figure 1. This location represented a shift in position from the standard MTR uranium core, also shown in Figure 1, which permitted the placement of eight fuel-follower shim rods in the core, thus increasing the control margin for this experiment.

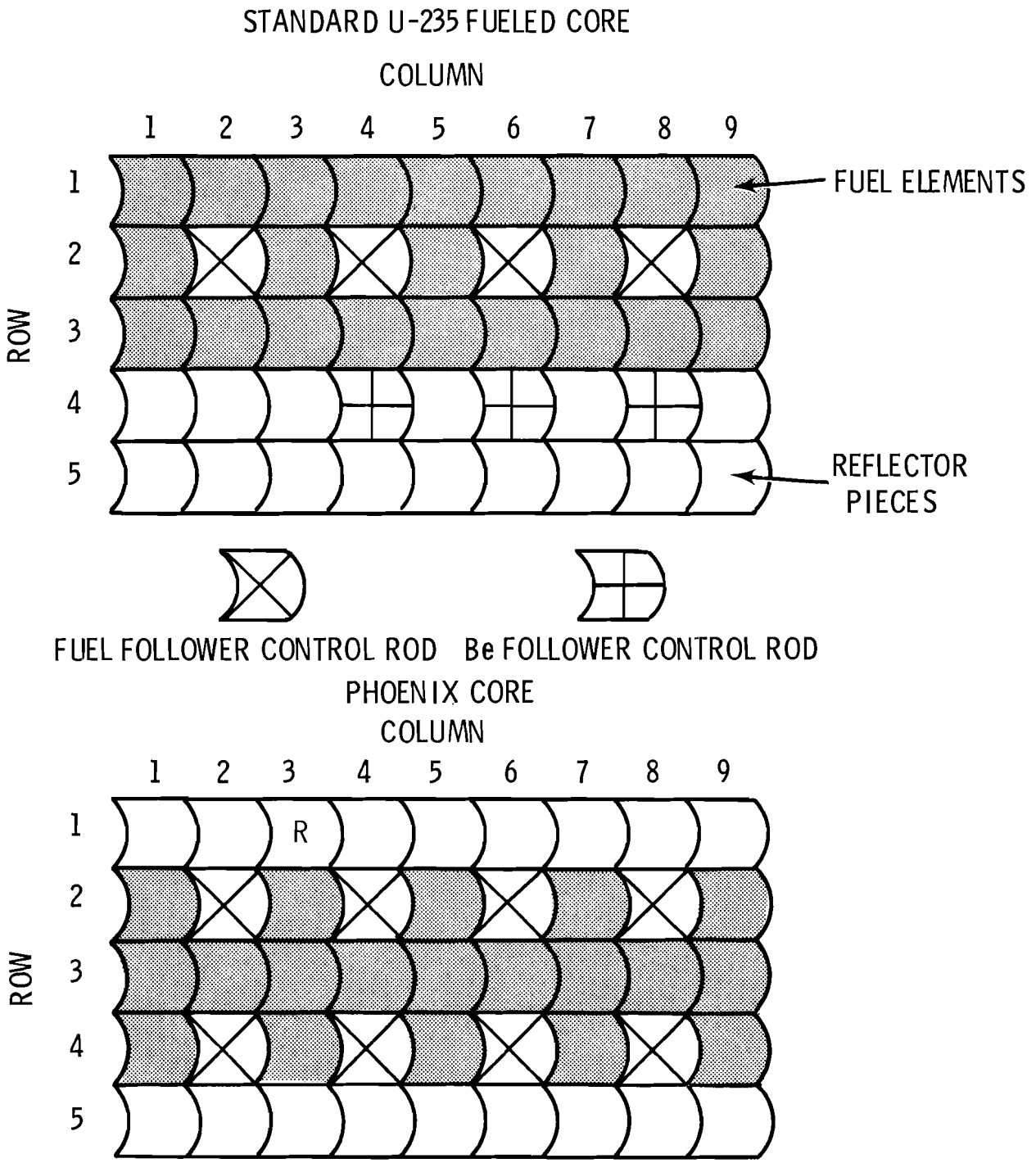

FIGURE 1. MTR Lattice Loadings for Standard and Phoenix Cores

III. THE MTR-PHOENIX FUEL BURNUP EXPERIMENT

A full-core burnup experiment is an expensive, time-consuming undertaking. However, it is the only effective way to evaluate the adequacy of methods and/or data being used in reactor calculations. The performance of the experiment in MTR has been reported previously[5]. Details of the core design and the power performance are repeated here to provide understanding of the experimental results and to facilitate an understanding of the computational problems associated with the burnup experiment analysis.

A. Core Description

The Materials Testing Reactor[6,7] is a rather heterogeneous assembly, with a plate-type core of aluminum alloy fuel that is moderated and cooled with light water, and reflected with beryllium, graphite and light water. The core measured approximately 9 inches north to south by 28 inches east to west by 24 inches high. Surrounding the core was a beryllium reflector which was 39 3/8 inches high and extended out to a diameter of 54 inches. Beyond this was a graphite reflector zone, which measured 12 feet north to south by about 15 feet east to west by 9 feet 4 inches high. The bottom of the graphite was located 4 feet below the core horizontal centerline.

The Phoenix Fuel core consisted of 19 fuel elements and 8 fuel-follower shim-safety rods located in the central 3 rows of the 5 x 9 lattice in the MTR, as shown in Figure 1. This location represented a shift in position from the standard MTR uranium core, also shown in Figure 1, which permitted the placement of eight fuel-follower shim rods in the core, thus increasing the control margin for this experiment.

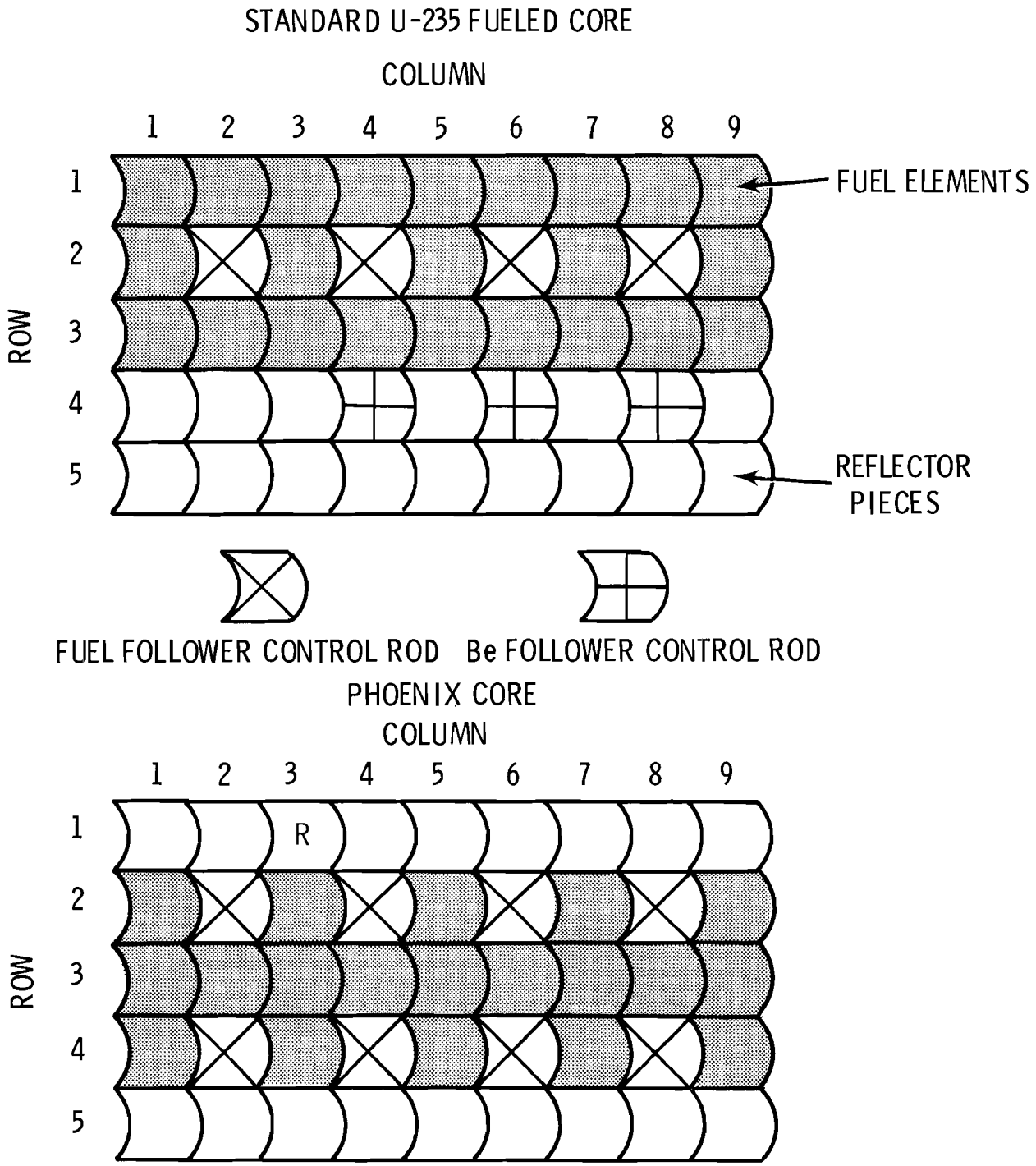

FIGURE 1. MTR Lattice Loadings for Standard and Phoenix Cores

The Phoenix fuel element illustrated in Figure 2, was similar in design to the standard MTR fuel element in that all external dimensions were the same. Internally, the Phoenix element consisted of sixteen 0.080 inch thick, equally spaced plates curved to the MTR configuration. Each plate contained a 0.040-inch thick alloy core composed of 21 wt% plutonium and 79 wt% aluminum. The fuel cores were clad with 6061 aluminum, 0.020 inches thick.

Five of the elements were modified to contain flux monitor wands inserted down the inside corner beside the side plate and between the second and third fuel plates from the concave side and extending the full length of the plates. These wands, illustrated in Figure 3, were Phoenix Fuel wires, co-extruded with 1100 series aluminum clad, with end pieces welded on. The fuel content of each was nominally 0.4 grams, and had the same isotopic composition as the fuel plates. The two fuel plates adjacent to the wand location in the flux monitor assembly had narrower fuel cores than the standard plates, as shown in Figure 3. The cores of the standard fuel plates contained 24.4 ± 1.2 grams of plutonium while those for the narrow core plates contained 21.0 ± 1.1 grams of plutonium. The finished Phoenix fuel element contained 390 ± 5 grams of plutonium and the flux monitor element contained 384 ± 5 grams of plutonium.

The Phoenix shim safety (control) rods were physically similar to the standard MTR shim control rods with the only exception being the thicker fuel plates in the fuel section. All remaining components (armature assembly, upper and lower aluminum sections, cadmium insert section, shock section, and associated hardware) were standard MTR components.

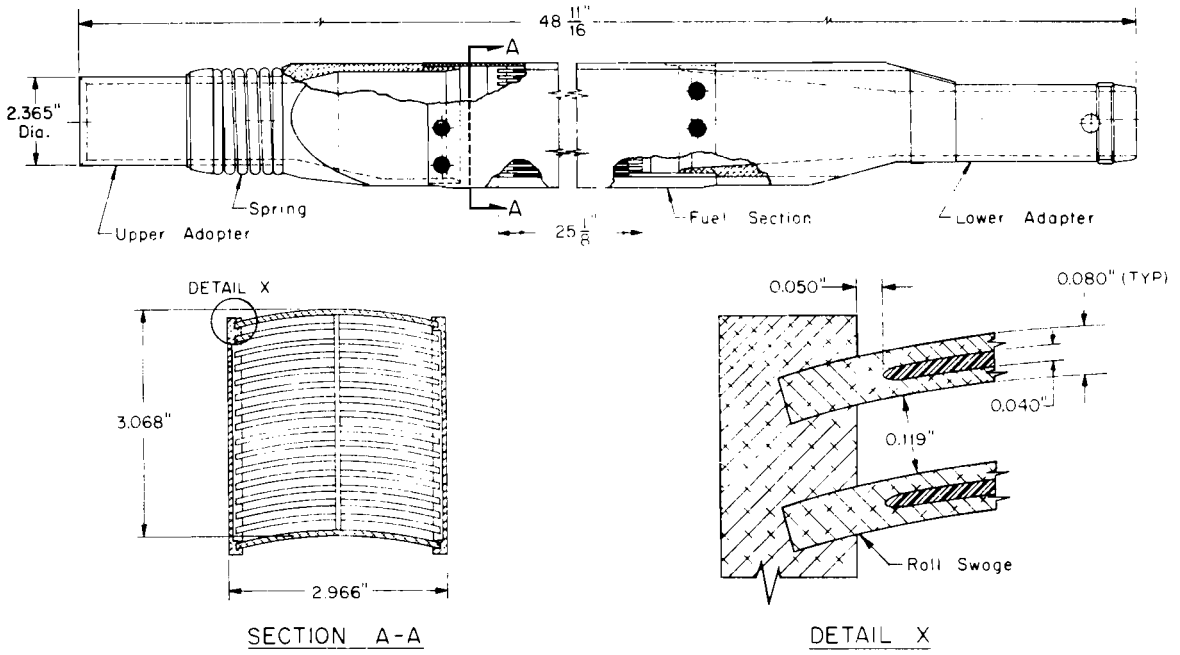

PHOENIX MTR FUEL ASSEMBLY

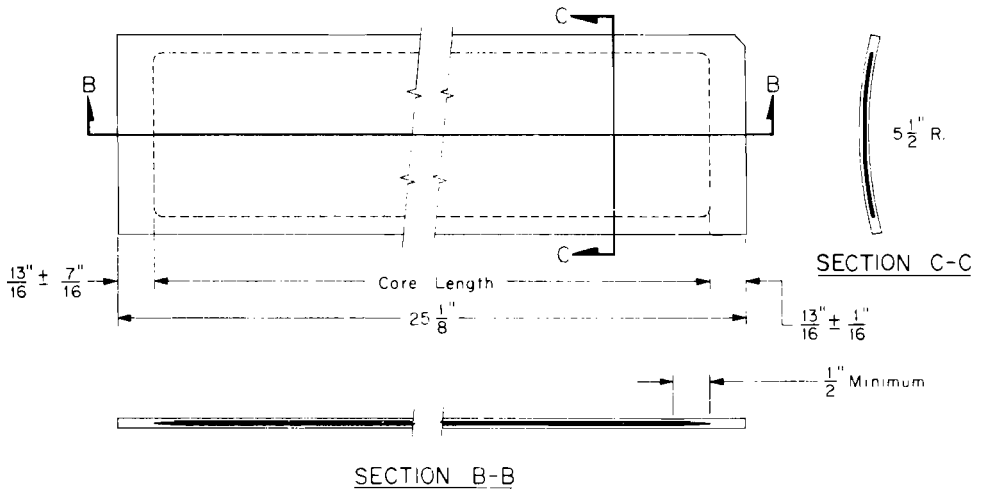

PHOENIX FUEL PLATE

FIGURE 2. MTR-Phoenix Fuel Element and Plate

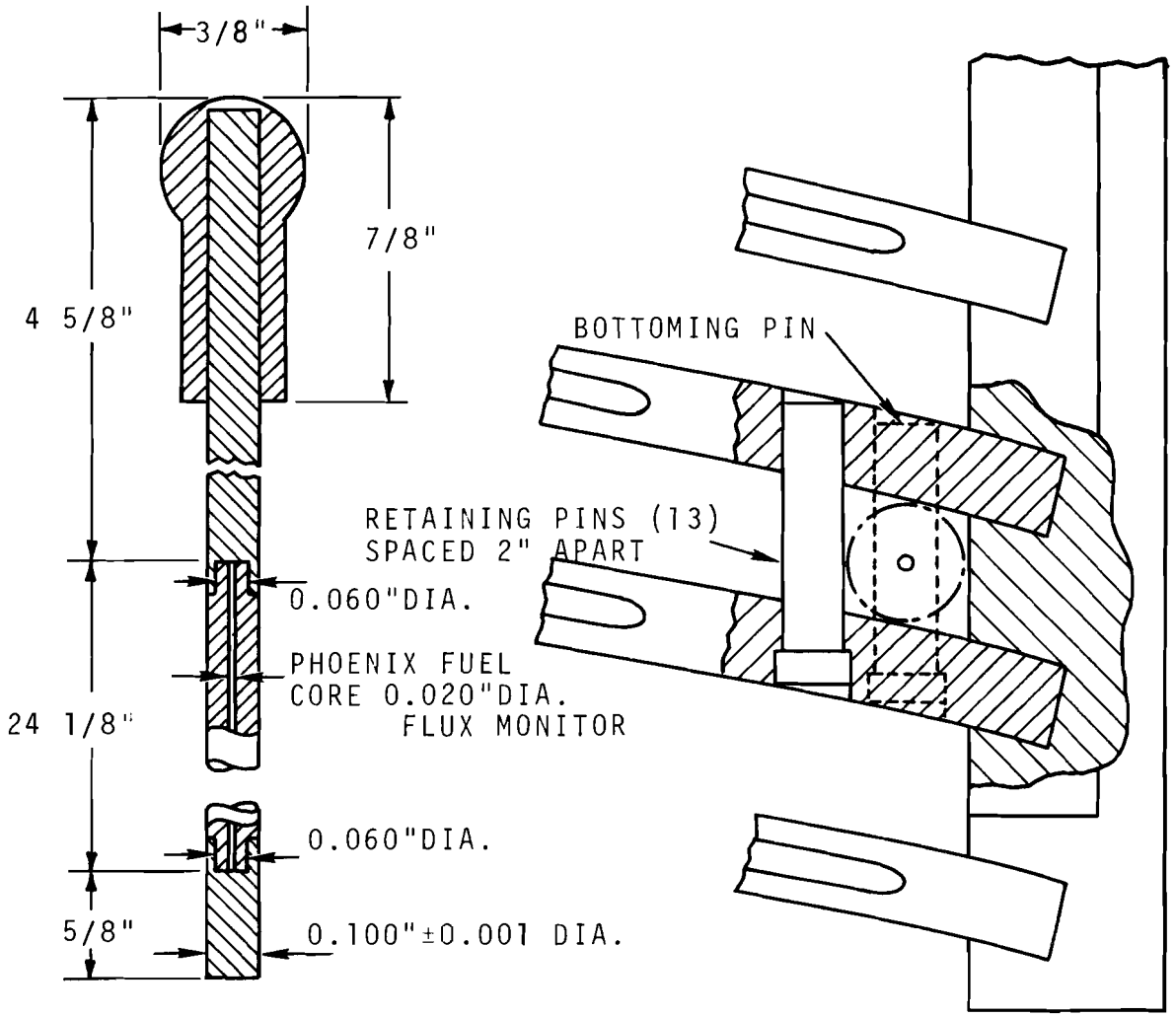

FIGURE 3. MTR-Phoenix Fuel Element with Flux Monitoring Position and Flux Monitor

The fuel section of the Phoenix shim safety rod consisted of thirteen 0.080-inch thick plates of standard MTR configuration spaced with 0.110-inch water channels. The fuel plates utilized the same 0.040-inch thick alloy cores composed of 21 wt% plutonium and 79 wt% aluminum as were used in the regular Phoenix fuel elements. The plutonium loading was 22.9 ± 1.1 grams per plate, or 298 ± 4 grams for the fuel section of one shim safety rod.

The isotopic composition of the plutonium used in the plates was measured in January of 1967. These values, adjusted to account for decay of ^{241}Pu into ^{241}Am between January, 1967 and the start of the burnup experiment in January of 1970, are presented in Table I.

TABLE I

ISOTOPIC COMPOSITION OF PLUTONIUM IN PHOENIX FUEL[a]

Pu Isotope	Atom % in Total Pu
238	0.539 ± 0.007
239	66.516 ± 0.055
240	23.201 ± 0.052
241	6.488 ± 0.034
242	3.257 ± 0.032

(a) Valued adjusted for ^{241}Pu decay to January, 1970.

B. Operating History During the Burnup Experiment

The operating history of the Phoenix fuel core in MTR is illustrated in Figure 4. Initial power operation began on January 28, 1970 and continued at various power levels until April 23, 1970, at which time a core burnup of 923 megawatt days had been achieved. The reactor was operated on a continous basis during the first five weeks of the experiment, and on a 24 hours/day-five day week for the remainder of the program.

The normal mode of equilibrium power operation was to compensate for the gradual loss of reactivity by moving the regulating rod from its least reactive position to its most reactive position. The regulating rod was then returned to its least reactive position in conjunction with a withdrawal of the banked shim-safety rods. During steady operation these rods were always operated as a bank. Rod bank height positions were measured at equilibrium power and fission product poisoning as a function of core burnup. The shim rod bank height data were interpreted through measured calibrations of the shim rods to obtain values of the rods-out $k_{effective}$ throughout the core burnup. These values are illustrated in Figure 5 and are compared with calculations in Section IV-C.

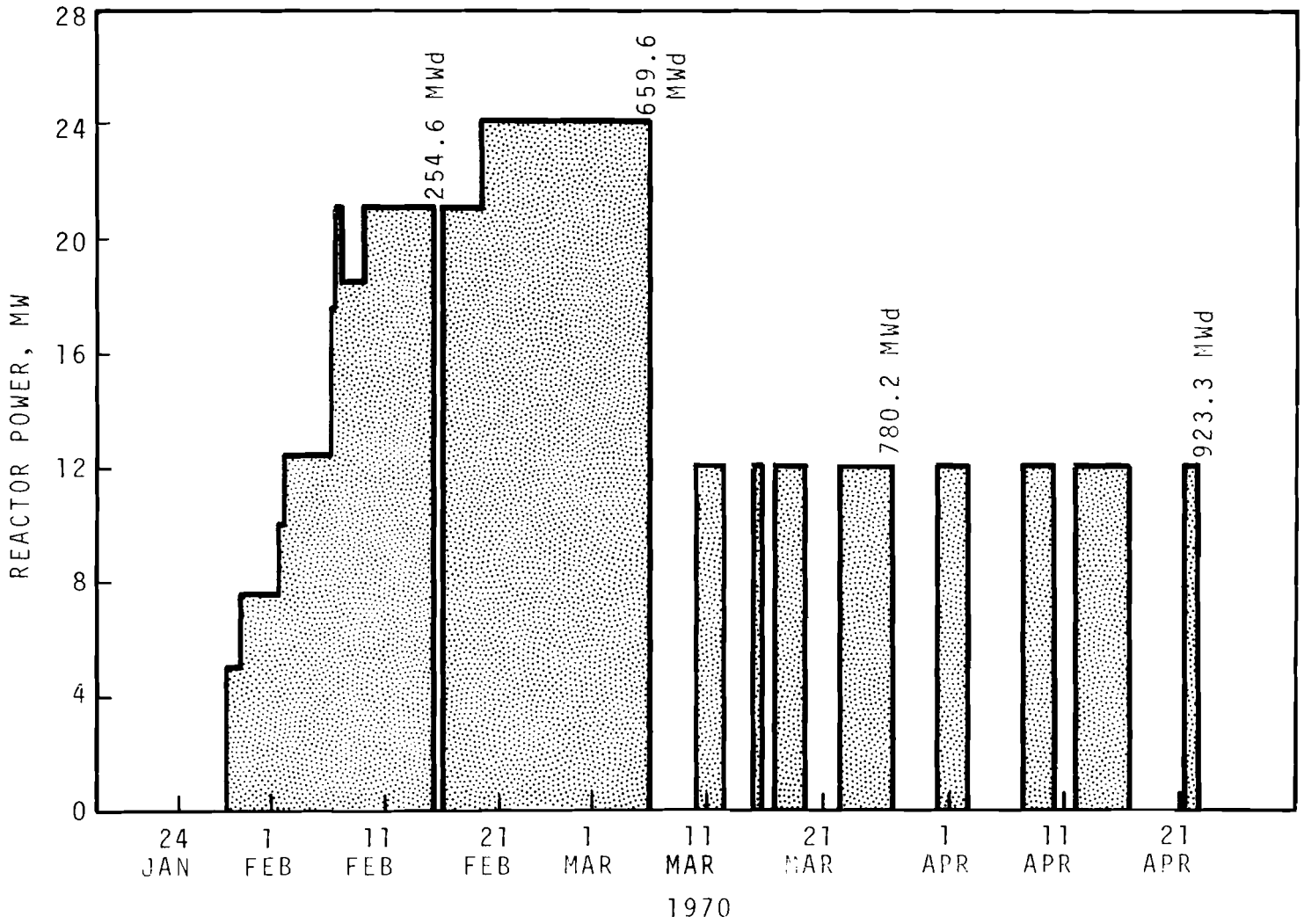

FIGURE 4. MTR-Phoenix Core Power History

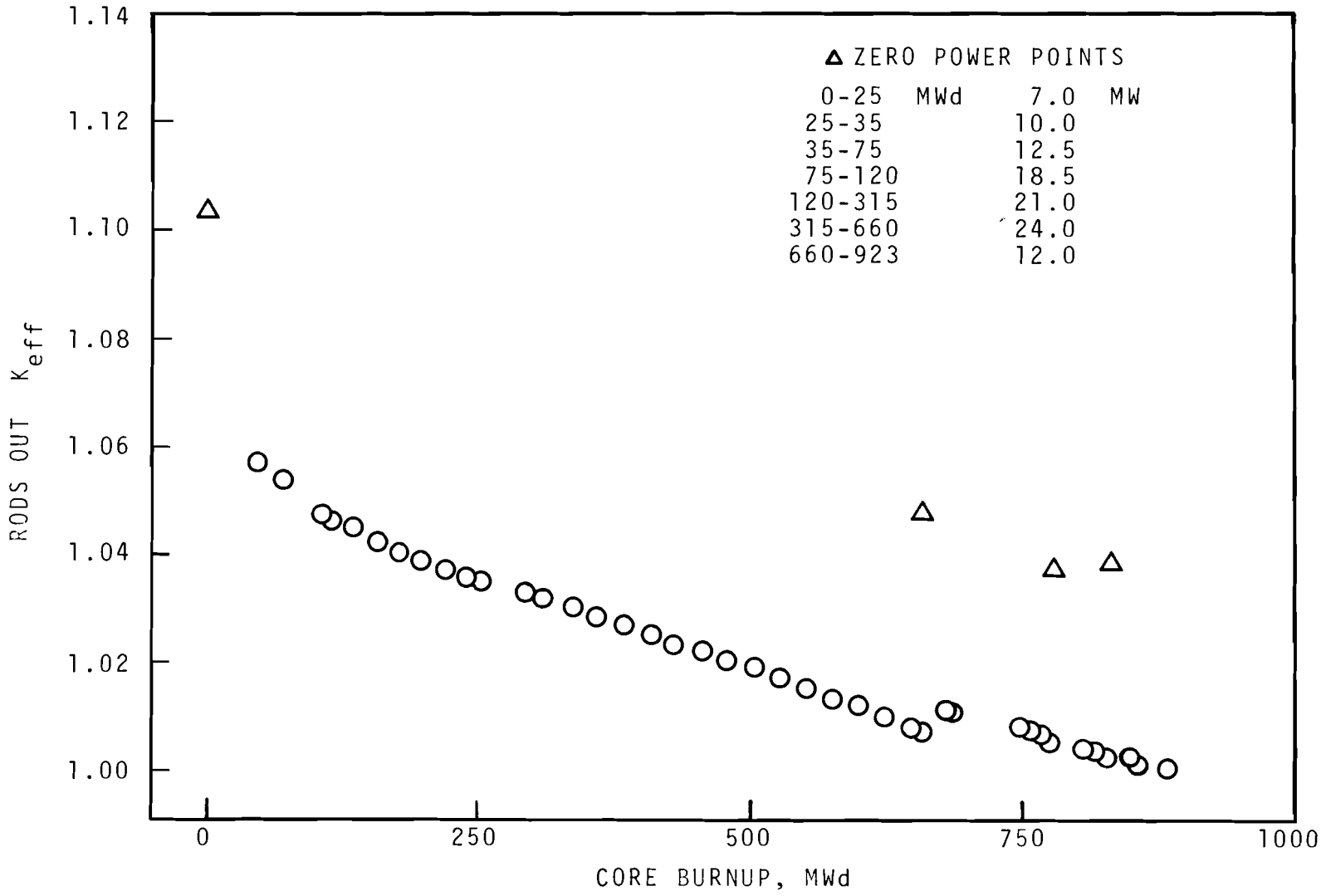

FIGURE 5. Rods-Out k_{eff} vs. MTR-Phoenix Core Burnup

C. Burnup Monitoring

The total power lifetime, and the beginning and ending isotopic compositions and power distributions are the primary quantities obtained from a burnup experiment. There are important advantages to also obtaining these data at intermediate steps during the burnup of the core. The fuel element design for MTR would not permit removal of any fuel plates before completion of the experiment. Therefore, fueled wands were designed which could be removed in order to obtain information at the intermediate burnup levels.

1. Flux Wands

The wands, described in Section III-A and illustrated in Figure 3, were located throughout the core as shown in Figure 6. The in-core history of each wand is listed in Table II. A single wand was removed

TABLE II

FLUX WAND HISTORY IN MTR-PHOENIX CORE

Wand No.	Fuel Element	Core Position	Date Removed	Core MWd At Removal
4	MP-11F	L-23	2-16-70	255 MWd
12	MP-12F	L-33	3-6-70	660 MWd
5	MP-13F	L-39	4-17-70	907 MWd
8	MP-14F	L-38	4-17-70	907 MWd
11	MP-10F	L-32	4-17-70	907 MWd

XX CORE POSITION
AA-XX ELEMENT NO.
XXX.X Pu-GRAMS
■ FLUX WAND NO.

21 MP-23 393.6	22 SHIM NP-7 297.8	23 MP-11F 380.3 ■4	24 SHIM NP-5 298.0	25 MP-6 392.3	26 SHIM NP-3 297.8	27 MP-8 393.8	28 SHIM NP-4 298.0	29 MP-16 393.3	3144.9g
31 MP-19 387.2	32 MP-10F 384.5 ■11	33 MP-12F 386.6 ■12	34 MP-4 394.4	35 MP-22 393.3	36 MP-2 393.2	37 MP-1 389.2	38 MP-14F 384.0 ■8	39 MP-13F 383.3 ■5	3495.7g
41 MP-17 392.7	42 SHIM NP-8 298.0	43 MP-7 394.6	44 SHIM NP-8 298.0	45 MP-3 389.7	46 SHIM NP-2 298.0	47 MP-9 392.4	48 SHIM NP-1 297.0	49 MP-18 396.3	3156.8g
1173.5g	980.3g	1161.5g	990.4g	1175.3g	989.1g	1175.4g	970.g	1172.9g	9797.4g TOTAL Pu WEIGHT

MTR-PHOENIX FUEL EXPERIMENT, ELEMENT NUMBER AND Pu WEIGHT IN GRAMS FOR THE CORE AS LOADED INTO THE MTR

FIGURE 6. Phoenix Fuel Experiment-MTR Core Loading

at each of two intermediate burnup levels, and three wands were removed just prior to the completion of the experiment. After cooling for about seven months, each wand was scanned in the PNL Gamma Scan Facility to obtain the axial burnup distributions shown in Figure 7. Gamma-ray spectra were obtained at selected locations on each wand, using a high resolution lithium-drifted germanium detector.

Three samples were cut from each of wands 8 and 12, at the locations shown in Figure 7. These six samples, together with a sample from an unirradiated wand, were analyzed to obtain isotopic compositions of plutonium, neodynium, and cesium. Concentrations of ^{137}Cs were determined as well as specific activities of selected fission products. The detailed results of these analyses are contained in Appendix A, with a summary of the data given in Table III. Comparisons of these results with calculation are contained in Section IV-B.

2. Fuel Plates

Following the burndown of the core, a total of forty-eight plates, four each from twelve elements, were removed for further examination and analysis. Thirty-six of the plates from nine different elements were gamma scanned to obtain axial and lateral burnup profiles. The scans of plates number 8 from elements MP-3, 6 and 22 are shown in Figures 8 and 9 as examples. These scans show the lateral and vertical burnup distribution across the central plane of the core, and show the large peaking that occurred at the lateral core-reflector interface.

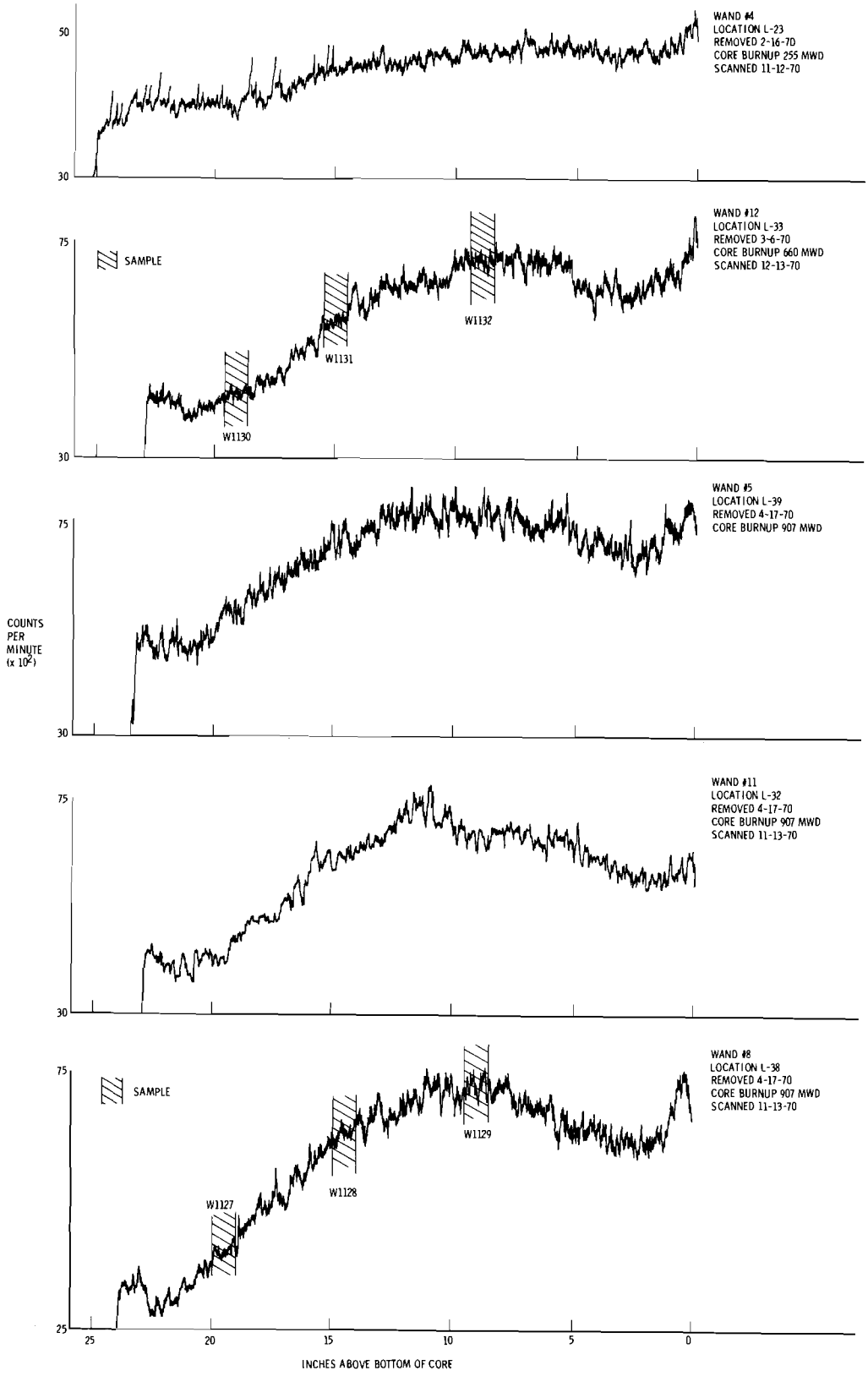

FIGURE 7. Axial Burnup Profiles from Flux Monitor Wands

TABLE III

SUMMARY OF DESTRUCTIVE ANALYSIS OF FLUX WAND SAMPLES

END OF LIFE ATOM CONCENTRATIONS (EOL)[b][c]

	Beginning of Life Concentrations (BOL)[a]	Wand No. 12			Wand No. 8		
Sample No.	W1126	W1130	W1131	W1132	W1127	W1128	W1129
^{238}Pu	0.539	0.5788	0.6147	0.6394	0.6148	0.6585	0.6819
^{239}Pu	66.516	58.94	52.58	47.93	54.31	45.10	42.67
^{240}Pu	23.201	23.13	22.93	22.42	22.94	22.41	21.94
^{241}Pu	6.488	8.227	9.612	10.63	8.999	10.76	11.26
^{242}Pu	3.257	3.441	3.629	3.797	3.556	3.932	4.023
Total	100.00	94.32	89.37	85.42	90.42	82.86	80.58
Atom % Burnup (BOL-EOL)	0	5.68	10.63	14.58	9.58	17.14	19.42
Atoms ^{137}Cs/Initial Pu Atom	0						
Atoms ^{148}Nd/Initial Pu Atom	0						

(a) BOL = atoms of isotope per 100 initial atoms of plutonium at beginning of life. (1-28-70)
(b) EOL - atoms of isotope per 100 initial atoms of plutonium at end of life (4-23-70)
(c) Values derived using measured isotopic ratios and ^{148}Nd analysis results in ISODIL.

The four locations which were sampled for destructive analysis are indicated in Figures 8 and 9, two from the interior of the core and two from the core boundary region. As with the flux wands, isotopic compositions of plutonium, neodynium and cesium were obtained, together with the specific activities of selected fission products. The detailed results of these analyses are contained in Appendix B, with a summary of the data given in Table IV. Comparisons of these data with calculations are contained in Section IV-B.

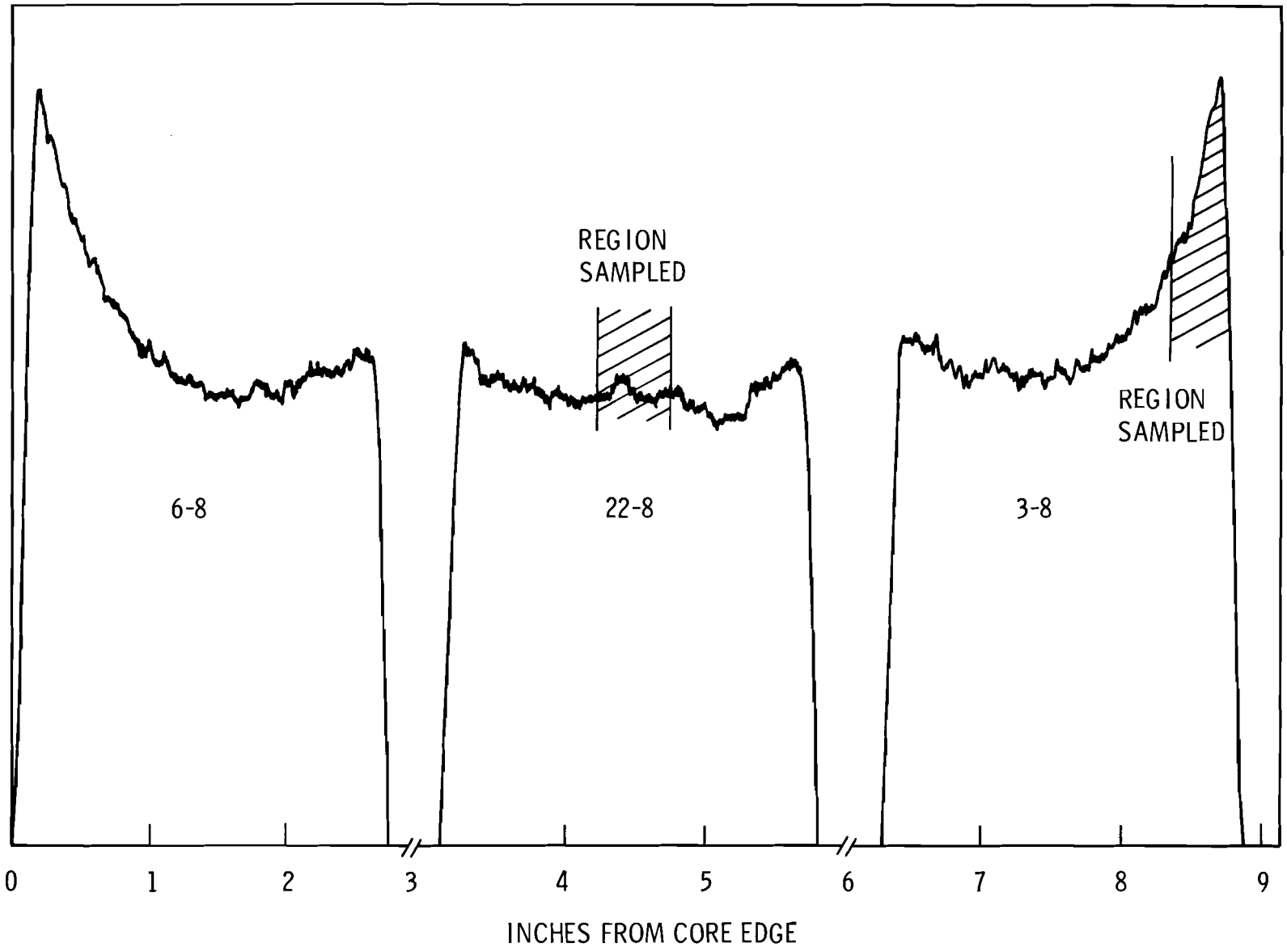

FIGURE 8. Horizontal Burnup Profile from Fuel Plates

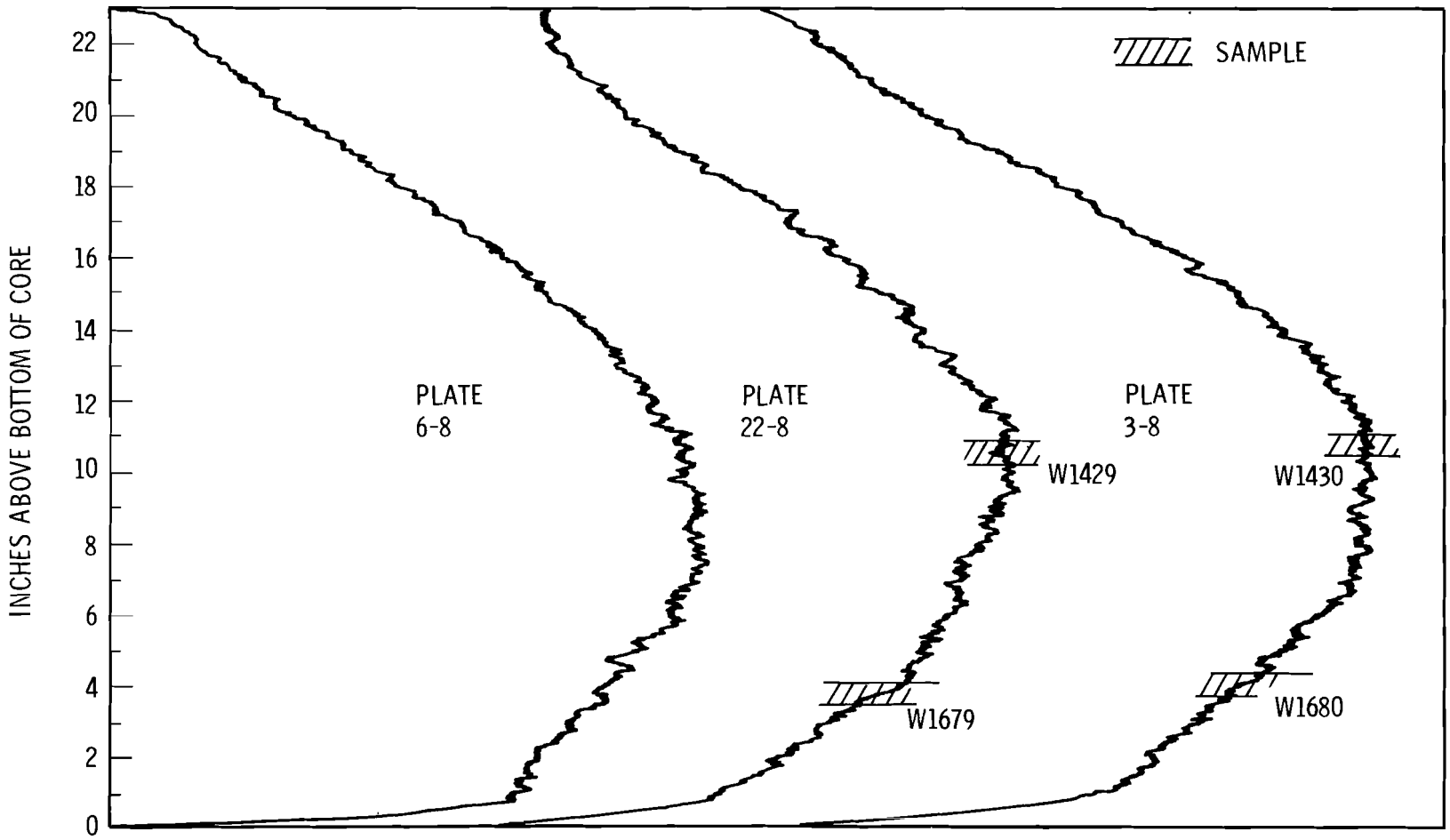

FIGURE 9. Axial Burnup Profile from Fuel Plates

TABLE IV

SUMMARY OF DESTRUCTIVE ANALYSIS OF FUEL PLATE SAMPLES

END OF LIFE ATOM CONCENTRATION (EOL)[b][c]

	Beginning of Life from Concentration (BOL)[a]	Plate 22-8		Plate 3-8	
Sample No.	W1126	W1429	W1679	W1430	W1680
^{238}Pu	0.539	0.7091	0.6855	0.6987	0.6979
^{239}Pu	66.516	48.84	50.78	41.39	44.17
^{240}Pu	23.201	24.04	24.09	25.02	25.18
^{241}Pu	6.488	9.344	9.004	8.892	8.477
^{242}Pu	3.257	3.688	3.641	4.085	3.962
Total	100.00	86.62	88.20	80.09	82.50
Atom % Burnup (BOL-EOL)	0	13.38	11.80	19.92	17.50
Atoms ^{137}Cs/Initial Pu Atom	0	9.0570×10^{-3}[d]	7.8351×10^{-3}[e]	1.3274×10^{-2}[d]	1.1708×10^{-2}[e]
Atoms ^{148}Nd/Initial Pu Atom	0	2.2965×10^{-3}	2.0413×10^{-3}	3.4276×10^{-3}	3.0321×10^{-3}

(a) BOL = atoms of isotope per 100 initial atoms of plutonium at beginning of life (1-28-70)
(b) EOL = Atoms of isotope per 100 initial atoms of plutonium at end of life (4-23-70
(c) Values derived using measured isotopic ratios and ^{148}Nd analysis results in ISODIL
(d) Values determined on 4/30/71
(e) Values determined on 6/24/71.

3. Measured Fission Product Data

Concentrations of selected fission products were measured in fuel plates and wands by both nondestructive and destructive techniques. The nondestructive method utilized a high resolution lithium-drifted germanium (Ge-Li) detector to determine gamma ray activities from the fission products photopeak areas. Typical gamma ray energy spectrum is shown in Figure 10. The energies and sources of the numbered photopeaks and the measured relative net photopeak areas for the various samples are listed in Table V.

Gamma spectrometric analysis (without chemical separation) was also performed on the dissolved plate and wand samples. Absolute specific activites of the same eight fission products studied in the nondestructive measurements were determined, with the results also listed in Table V. In addition, the ^{137}Cs activity in some of the samples was determined by direct gamma ray spectrometry after a chemical separation. These values were determined by comparison with a calibrated ^{137}Cs source, and are listed in Tables III and IV.

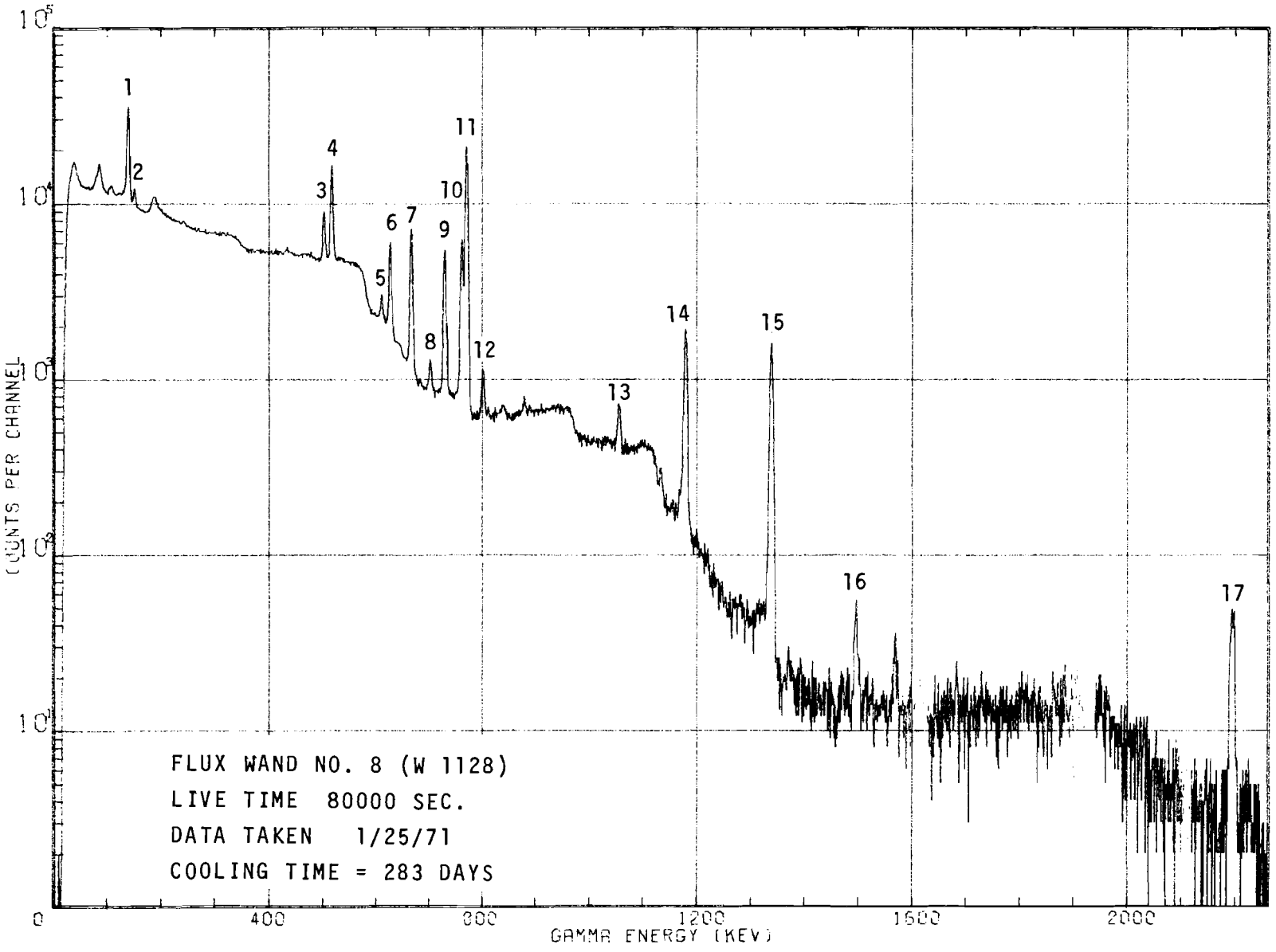

FIGURE 10. Typical Gamma-ray Spectrum from a Flux Wand

TABLE V

RELATIVE NET PHOTOPEAK AREAS, MEASURED USING A GeLi DETECTOR SYSTEM

Peak Number	Energy (Kev)	Source	W1130 (1-19-71)	W1131 (1-20-71)	W1132 (1-21-71)	W1127 (1-22-71)	W1128 (1-25-71)	W1129 (1-26-71)	W1430 (4-14-71)	W1680 ( )	W1429 (4-15-71)	W1629 ( )
1	135	^{144}Ce	178	241	282	228	323	331	1251		943	
2	147	^{141}Ce	70	89	101	95	117	114	198		150	
3	496	^{103}Ru	72	103	118	110	141	145	292		223	
4	512	^{106}Ru-^{106}Rh	134	183	213	171	234	249	931		696	
5	605	^{134}Cs	37	40	49	39	59	65	274		199	
6	622	^{106}Ru-^{106}Rh	80	112	130	104	144	151	543		403	
7	662	^{137}Cs	51	84	100	83	117	125	505		377	
8	693	^{144}Ce	25	36	40	37	46	49	175		131	
9	724	^{95}Zr	84	115	131	116	152	159	416		316	
10	757	^{95}Zr	203	277	315	271	360	377	443		338	
11	766	^{95}Nb	161	225	256	227	283	313	882		668	
12	796	^{134}Cs	29	36	42	35	51	55	223		160	
13	1050	^{106}Ru-^{106}Rh	23	30	38	28	39	45	101		72	
14	1173	^{60}Co	--	--	--	--	--	--	160		118	
15	1332	^{60}Co	--	--	--	--	--	--	78			
16	1489	^{144}Ce	7	11	15	11	16	16	29		25	
17	2186	^{144}Ce	11	13	16	13	18	19	31		20	

		(2-22-71)	(5-6-71)	(6-22-71)	(5-6-71)	(6-22-71)
Specific Activities in Dissolved Samples (dis/sec/Initial Pu Atom)	^{144}Ce		7.516(-11)	5.404(-11)	5.005(-11)	3.825(-11)
	^{141}Ce		<3.572(-13)	4.966(-14)	<1.850(-L3)	9.936(-14)
	^{103}Ru		1.700(-12)	5.142(-13)	1.043(-12)	3.565(-13)
	^{106}Ru-^{106}Rh		9.136(-11)	6.752(-11)	6.114(-11)	4.727(-11)
	^{134}Cs		1.867(-12)	1.272(-12)	1.193(-12)	8.981(-13)
	^{137}Cs		9.273(-12)	7.264(-12)	6.086(-12)	5.174(-12)
	^{95}Zr		1.138(-11)	5.232(-12)	6.892(-12)	3.731(-12)
	^{95}Nb		2.975(-11)	9.247(-12)	1.853(-11)	6.448(-12)

IV. THEORY-EXPERIMENT COMPARISONS

Since the primary purpose of a burnup experiment is to obtain data with which to test and evaluate current and future computational methods and cross section data, it is important in any comparisons of the experiment with theory to carefully delineate the models, methods and data used in the calculations. Descriptions are given in the following sections of the core models, cell, reactor and burnup codes and cross section data used to calculate the MTR-Phoenix Fuel experiment. Comparisons are made between experimental and calculated ratios of effective cross sections, derived from isotopic data, and between measured and calculated rates of reactivity loss with burnup. The sensitivity of the calculated results to details within the models is examined and reasonable limits of uncertainty are defined.

A. Calculational Models and Methods

The core geometry in MTR is rather complex and necessitates making a number of simplifying assumptions to stay within the capacities of current reactor codes. The unit cell used in the thermal cross section generating code BRT-1[8] consisted of a repeating slab array of fuel, cladding and water. The cross sections generated using this simple cell model are appropriate for the asymptotic region of the core. Unfortunately, due to the small size and large surface to volume ratio of the core, less than 80% of the core is in the asymptotic region. At least 20% of the fuel in the core is in the core-reflector boundary zone, where the thermal neutron spectrum is changing rapidly with position. In core calculations in general and in burnup calculations in particular, the entire core was considered as

being in the asymptotic spectrum. The results of the destructive analyses of fuel plates, presented in Section III-C, show that this assumption is not valid and that serious errors in estimating cross sections and isotopic compositions will result. Nevertheless, in all calculations reported in this report, the assumption of an asymptotic spectrum was made, unless otherwise specified.

1. Description of Computational Models

The majority of the calculations made for comparison with the experimental results from the MTR Phoenix fuel program were performed using the ZODIAC-G code.[9] This code is an automated chain consisting of THERMOS[8] for the thermal group cell calculation, HRG[10] for the epithermal cell calculation, HFN[11] for the one-dimensional reactor calculation and ALCHEMY[12] for the reactor burnup calculation.

The fuel plate unit cell used in THERMOS consisted of the following: a reflecting boundary, 0.020 inches (0.0508 cm) of fuel alloy, 0.020 inches (0.0508 cm) of aluminum cladding, 0.0593 inches (0.13062 cm) of water, and a reflecting boundary. These three regions were homogenized per HRG, with heterogeneity effects introduced by means of resonance parameters and a mean chord length. The atom densities for materials used in the cell calculations are listed in Table VI.

The reactor calculation in ZODIAC-G uses the one-dimensional multigroup diffusion code HFN. The core volume assumed in the calculation was 7.1956×10^4 cm^3, based on the cell atom densities and the total plutonium in the core. A value of 9753 g of plutonium was used, as had been assumed in the MTR-Phoenix SAR, rather than the actual value of 9797.4 g as loaded. The saturating fission product poisons ^{135}Xe and ^{149}Sm

TABLE VI

ATOM DENSITIES FOR CELL CALCULATIONS

(Atoms per barn-centimeter)

Material	BRT-1	HRG[c]
^{239}Pu	1.10754×10^{-3}	2.2307×10^{-4}
^{240}Pu	3.9422×10^{-4}	7.9400×10^{-5}
^{241}Pu[a]	1.1355×10^{-4}	2.287×10^{-5}
^{242}Pu	5.905×10^{-5}	1.1893×10^{-5}
^{241}Am[b]	1.757×10^{-5}	3.54×10^{-6}
Aluminum		
H_2O		

(a) Corrected for ^{241}Pu decay between time of separation and start of power operation.

(b) Resulting from ^{241}Pu decay between time of separation and start of power operation.

(c) No spatial fine structure in HRG, all materials smeared over total cell volume.

were included explicitly, but ^{105}Rh was not. A single pseudo fission product was used to represent the nonsaturating fission products, based on a yield-weighted combination of the Nephew pseudo fission products,[13] using the yields compiled by Nephew.

The version of HRG used in the ZODIAC-G chain (HRG3) provided for allocation of a number of fine energy groups around the 1 eV resonance in ^{240}Pu, and had a treatment for intermediate resonances in the presence of an admixed scatterer. No upscattering was included, however. The ^{241}Am which was produced by decay of ^{241}Pu was included explicitly, but no other transplutonium isotopes were considered. A reactor power level of 24 MW was assumed during the burnup, and the isotopic concentrations were recomputed every five full power days, once the saturating fission products were in equilibrium. Spectrum-averaged cross sections were recomputed every fifteen full power days.

B. Comparisons of Measured and Calculated Isotopic Concentrations

One measure of the adequacy of a calculational method is its ability to predict the variations in isotopic compositions with fuel burnup that are actually encountered in the reactor core. Because of the complexity of the MTR-Phoenix core, it was anticipated that this experiment would provide a very severe test of the computational methods, and special efforts were made to obtain data appropriate for these comparisons.

1. Measured Isotopic Data

As described in Section III-C, the MTR-Phoenix core contained fueled wands which could be removed at intermediate levels of burnup. Samples from the wands and from fuel plates removed at the end of core

life were analyzed to obtain plutonium isotopic concentrations and fission product concentrations for various stages of burnup. The number of fissions that occurred in each sample were determined via analyses of the ^{148}Nd and ^{137}Cs contents, to obtain the atom percent burnups in each sample. The agreement between the results using the two different fission product monitors was generally good, with the numbers of fissions indicated from the ^{137}Cs analysis being slightly (<3%) but systematically greater than that indicated from the ^{148}Nd analysis.

The isotopic data, presented previously in Tables III and IV, are shown graphically in Figures 11a through 11d, where the ratio of End-of-Life to Beginning-of-Life numbers of atoms is plotted for ^{239}Pu, ^{240}Pu, ^{241}Pu and ^{242}Pu versus atom percent burnup of total initial plutonium. The solid line in all figures is the result predicted by a ZODIAC-G burnup calculation.

An excellent agreement between measured and calculated values of ^{239}Pu depletion as a function of atom percent burnup is seen in Figure 11a. Indications of different burnup paths for the plates and the wands begin to appear in Figure 11b, where the calculation under-predicts the ^{240}Pu content of the plates and overpredicts the ^{240}Pu content of the wands. Examination of Figure 11c suggests that the interior region of the core was on a different burnup path from the exterior region, and that both plates were different from the wand samples. No clear-cut differences are seen between the paths of the various samples in Figure 11d where the variation in ^{242}Pu concentration with burnup is shown, but the calculation consistently under-predicts the ^{242} concentration.

Several plausible arguments can be advanced to explain the observed variations in isotopic concentrations. First, the neutron spectrum in

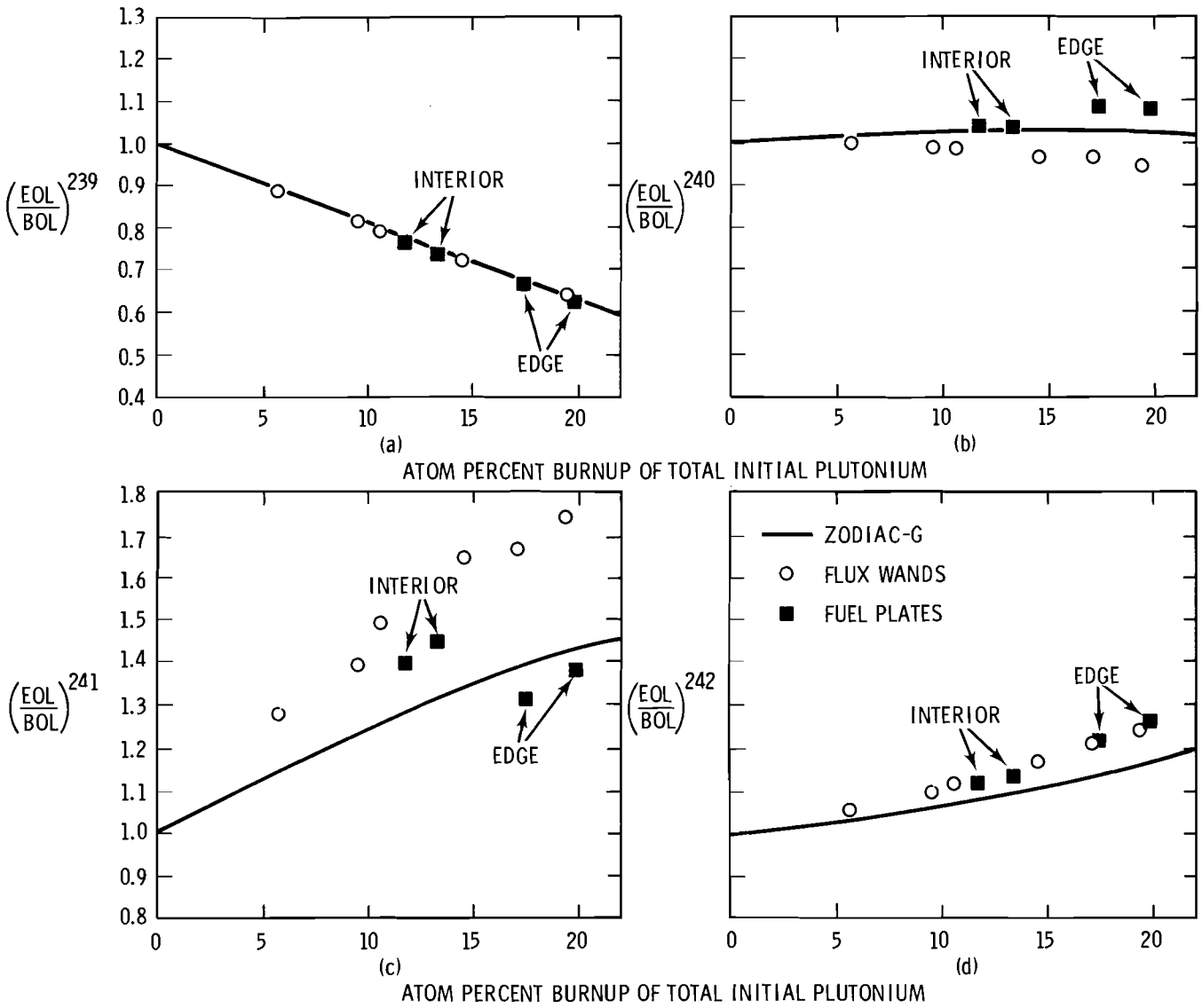

Figure 11. Comparison of the Ratios of Pu Isotopic Concentration at Beginning of Life to End of Life as a Function of Burnup of Total Initial Plutonium, Measured and Calculated.

the core interior is less thermalized than at the core edge. Second, the ^{240}Pu resonance self-shielding is less in the wands due to the smaller thickness relative to the plates. A factor of 1.8 has been calculated as the ratio of the effective resonance integrals of the 0.020 inch diameter wand core to the 0.040 inch thick plate core, which influences the removal rate of ^{240}Pu and the production rate of ^{241}Pu. A more detailed examination of the effect of the neutron spectrum and core geometry on the effective cross sections of the Phoenix fuel is given in the following section.

2. Ratios of Effective Cross Sections

While the variations of the isotopic concentration of plutonium are an important experimental result, these variations are not very sensitive indicators of where the computational problems lie. However, these experimental data can be used in an analysis technique[14] to obtain ratios of effective cross sections which can be compared with values of the same ratios calculated by any particular computational system. One can readily observe the ratios which differ from experiment and can examine the methods, data, etc., used in the calculations that will influence the discrepant result.

If one examines the one-group transmutation equations, shown below,

$$\frac{dN^i}{dt} = -\lambda^i N^i \rightarrow \hat{\sigma}_o^i N^i \phi + \hat{\sigma}_c^{i-1} N^{i-1} \phi$$

$$\frac{dN^j}{dt} = - \hat{\sigma}_a^j N^j \phi$$

he finds that the parameters most difficult to determine in a burnup experiment are the flux, ϕ, and the time, t. If the firs equation is divided by the second equation, these parameters are cancelled (except for a relatively insignificant term for which a reasonable estimate of the flux will be sufficient).

$$\frac{dN^i}{dN^j} = \frac{\lambda^i N^i}{\hat{\sigma}_a^j N^j \phi} + \frac{\hat{\sigma}_a^i N^i}{\hat{\sigma}_a^j N^j} - \frac{\hat{\sigma}_c^{i-1} N^{i-1}}{\hat{\sigma}_a^j N^j}$$

One obtains a set of equations that can be integrated and which are functions of the isotopic concentrations and the ratios of effective cross sections. Having the isotopic concentrations from a destructive analysis of the fuel, one can now fit this set of equations to the data using a multivariable non-linear least squares program[15] to obtain the ratios of effective cross sections.

3. Least Squares Analysis of Isotopic Data

The isotopic composition data for the flux wands and fuel plates were fitted by the least-squares code DBUFIT-I to determine ratios of average cross sections involved in the transmutation process.

The set of fitted equations is

$$N^{240} + AA/A + \frac{\varepsilon}{1-A} N^{239} - K_o (N^{239})^A = 0$$

$$N^{241} - \frac{\varepsilon A}{(1-A)(1-B)} N^{239} + \frac{AK_o}{A-B} (N^{239})^A - K_1 (N^{239})^B = 0$$

$$N^{242} + \frac{\gamma\varepsilon AB}{(1-A)(1-B)(1-C)} N^{239} - \frac{\gamma ABK_o}{(A-B)(A-C)} (N^{239})^A + \frac{\gamma BK_1}{B-C} (N^{239})^B - K_2 (N^{239})C = 0$$

$$N_f = -(1-\varepsilon)(N_o^{239} - N^{239}) + K_f + \left\{ \frac{1}{1+\lambda^{241}/\hat{\sigma}^{241}\phi} - \gamma \right\} \left\{ \frac{\varepsilon AB}{(1-A)(1-B)} N^{239} - \frac{BK_o}{A-B} (N^{239})^A + K_1 (N^{239})^B \right\} = 0,$$

where the parameters related to the cross-section ratios are

$$\varepsilon = \hat{\sigma}_c^{239}/\hat{\sigma}_a^{239}$$

$$A+AA/N^{240} = \hat{\sigma}_a^{240}/\hat{\sigma}_a^{239}$$

$$B = (\hat{\sigma}_a^{241}/\hat{\sigma}_a^{239})(1+\lambda^{241}/\hat{\sigma}_a^{241}\phi)$$

$$\gamma = (\hat{\sigma}_c^{241}/\hat{\sigma}_a^{241})/(1+\lambda^{241}/\hat{\sigma}_a^{241}\phi)$$

$$C = \hat{\sigma}_a^{242}/\hat{\sigma}_a^{239},$$

while K_o, K_1, K_2 and K_f are constants of integration dependent on the initial concentrations. Note that the factor $(1+\lambda^{241}/\hat{\sigma}_a^{241}\phi)$ corrects for the radioactive decay of ^{241}Pu.

In the DBUFIT-I code the parameter C is not permitted to vary. It must be fixed by independent considerations. Furthermore, since the concentration of ^{240}Pu is relatively constant during the burnup of Phoenix fuel, it is not feasible to determine AA, which expresses a (formal) concentration dependence of $\hat{\sigma}_a^{240}/\hat{\sigma}_a^{239}$. Thus AA was held fixed at zero in all runs. Summarizing then, we hope to determine four cross-section ratios, assuming that a fifth one is known from previous calculations.

The data for the samples from wands #12 and #8 were fitted first. Initially the data from both wands were combined and fitted as one case. In the remainder of this section, we use the abbreviations $r^n(\equiv\hat{\sigma}_a^n/\hat{\sigma}_a^{239})$ and $\alpha^n(\equiv\hat{\sigma}_c^n/\hat{\sigma}_f^n)$. The results for two different (fixed) values of r^{242} are shown in lines 1 and 2 of Table VII. After systematic differences between the wands were noticed, the data for each were fitted separately as shown in lines 3-6 of Table VII. The quality of the fits for the separate cases, as measured by χ^2/d.f., is significantly better than for the composite cases. (χ^2 is the inverse-variance-weighted sum of squares, and d.f. is the number of statistical degrees of freedom.) For both the separate and composite cases, these results show that only α^{241} is sensitive to the assumed value of r^{242}. In all cases the error estimates are rather large. This is a consequence of the high correlation among the 7 free parameters (4 cross-section ratios and 3 initial concentrations).

In anticipation of the sparse fuel plate data of main interest, a special set of fits were made in which only the initial and highest exposure wand data were used. The results are shown in lines 7-12 of Table VII. It turned out that physically plausible fits could not be obtained unless an additional constraint was imposed on the parameters. Since the ratio r^{241} is perhaps least sensitive to resonance integral and spectral errors, it was fixed at a set of values near those obtained from reactor calculations. These results show that all 3 of the free cross-section ratios are sensitive to the assumed value of r^{241}.

Unfortunately, the data for fuel plates #22-8 and #3-8 were rather sparse, consisting of only two closely spaced sets of isotopic concentrations for each plate after exposure in addition to the zero-exposure values. Thus, it was necessary to constrain the cross-section ratios in order to obtain physically plausible results, which are given in Table VIII. In all of these fits the ratios r^{241} and r^{242} were held fixed in a range of values obtained by reactor calculations. A preliminary set of fits had shown that the results obtained by fixing α^{241} and r^{242} are essentially equivalent to those obtained by fixing r^{241} and r^{242}.

Inspection of Table VIII indicates that to a good degree of approximation ($\sim$1%) the ratios α^{239}, r^{240}, and α^{241} may be considered as linear functions of r^{241} and r^{242}. The linear coefficients are best determined by a second-level least-squares fit to the tabulated values. For fuel plate #22-8 (asymptotic region) the resulting equations are:

$$\alpha^{239} = 0.557 + 0.340\ (r^{241}-1.05)-0.033(r^{242}-0.26)$$
$$r^{240} = 0.747 + 0.345\ (r^{241}-1.05)-0.017(r^{242}-0.26)$$
$$\alpha^{241} = 0.385 - 0.515\ (r^{241}-1.05)+0.767(r^{242}-0.26)$$

For fuel plate #3-8 (edge region) the equations are:

$$\alpha^{239} = 0.465 + 0.310\ (r^{241}-1.00)-0.025(r^{242}-0.12)$$
$$r^{240} = 0.522 + 0.320\ (r^{241}-1.00)$$
$$\alpha^{241} = 0.398 - 0.565\ (r^{241}-1.00)+0.900(r^{242}-0.12)$$

It should be pointed out that in Tables VII and VIII, the values of χ^2/d.f. distinctly tend to be smaller than the expected value of 1. This suggests the possibility of a systematic tendency to overestimate the errors of the input data.

Table VII. Results of Least-Squares Fits of Wand Data

Fuel Material	No. of Data Pts.	Cross-Section Ratios					
		α^{239}	r^{240}	r^{241}	α^{241}	r^{242}	χ^2/d.f.
Wands 12 & 8	7	0.604 ± 0.095	1.018 ± 0.090	1.329 ± 0.230	0.322 ± 0.081	0.361	2.68
Wands 12 & 8	7	0.601 ± 0.095	1.016 ± 0.091	1.326 ± 0.232	0.343 ± 0.088	0.400	2.73
Wand 12	4	0.529 ± 0.064	0.957 ± 0.069	1.064 ± 0.186	0.449 ± 0.119	0.361	0.484
Wand 12	4	0.533 ± 0.059	0.960 ± 0.064	1.069 ± 0.172	0.402 ± 0.095	0.300	0.412
Wand 8	4	0.446 ± 0.064	0.849 ± 0.073	0.945 ± 0.188	0.539 ± 0.173	0.361	0.928
Wand 8	4	0.449 ± 0.061	0.851 ± 0.070	0.947 ± 0.179	0.481 ± 0.142	0.300	0.841
Wand 12	2	0.485 ± 0.008	0.916 ± 0.006	0.950 fixed	0.475 ± 0.023	0.300	0.263
Wand 12	2	0.521 ± 0.009	0.955 ± 0.006	1.050 fixed	0.410 ± 0.020	0.300	0.277
Wand 12	2	0.559 ± 0.009	0.994 ± 0.006	1.150 fixed	0.361 ± 0.017	0.300	0.292
Wand 8	2	0.445 ± 0.008	0.856 ± 0.005	0.950 fixed	0.471 ± 0.020	0.300	0.323
Wand 8	2	0.483 ± 0.008	0.897 ± 0.006	1.050 fixed	0.407 ± 0.016	0.300	0.341
Wand 8	2	0.523 ± 0.009	0.939 ± 0.006	1.150 fixed	0.357 ± 0.014	0.300	0.360

Table VIII. Results of Least-Squares Fits of Fuel Plate Data

Fuel Material	No. of Data Pts.	Cross-Section Ratios					
		α^{239}	r^{240}	r^{241}	α^{241}	r^{242}	χ^2/d.f.
Plate 22-8	3	0.524 ± 0.005	0.713 ± 0.003	0.950 fixed	0.440 ± 0.014	0.260	0.153
Plate 22-8	3	0.557 ± 0.005	0.747 ± 0.003	1.050 fixed	0.382 ± 0.012	0.260	0.162
Plate 22-8	3	0.592 ± 0.006	0.782 ± 0.003	1.150 fixed	0.337 ± 0.011	0.260	0.172
Plate 22-8	3	0.558 ± 0.005	0.748 ± 0.003	1.050 fixed	0.359 ± 0.011	0.230	0.140
Plate 22-8	3	0.556 ± 0.006	0.747 ± 0.003	1.050 fixed	0.405 ± 0.013	0.290	0.187
Plate 3-8	3	0.434 ± 0.012	0.490 ± 0.006	0.900 fixed	0.459 ± 0.032	0.120	1.34
Plate 3-8	3	0.464 ± 0.012	0.522 ± 0.006	1.000 fixed	0.395 ± 0.026	0.120	1.34
Plate 3-8	3	0.496 ± 0.013	0.554 ± 0.006	1.100 fixed	0.346 ± 0.022	0.120	1.34
Plate 3-8	3	0.465 ± 0.012	0.522 ± 0.006	1.000 fixed	0.377 ± 0.025	0.100	1.33
Plate 3-8	3	0.464 ± 0.012	0.522 ± 0.006	1.000 fixed	0.413 ± 0.027	0.140	1.35

C. Reactivity Loss Rate Comparisons

The principal virtue expected of the Phoenix fuel concept was the ability to have an extended core lifetime without a large initial excess reactivity. Therefore, an important parameter to investigate was the rate at which the core excess reactivity was depleted during burnup, and to compare the measured rate with rates calculated by the computational models. Also, some useful insight can be obtained by comparing the measured reactivity loss rates for several earlier MTR cores with that of the MTR-Phoenix core.

1. Measured Reactivity Loss Rates

The basic characteristics of the Phoenix core, a standard ^{235}U core, an earlier plutonium core (cycle 108), and a 20% enriched U core are listed in Table IX. The experimental burnup results for those four cores are illustrated in Figure 12. The standard ^{235}U core operated at a constant power level of 40 MW while the other cores operated at various levels. during their lifetimes. The reactivity curve for each core has been corrected to a constant power level (30 MW for cycle 108 and the 20% enriched core, 24 MW for the Phoenix core). Since the curves of excess reactivity versus burnup are not linear, an average reactivity loss rate was computed by dividing the excess reactivity at 100 MWd burnup (assumes saturated fission product poisons) by the number of megawatt-days of core life beyond 100 MWd.

TABLE IX

Comparison of MTR-Phoenix Fuel Core with Previous MTR Cores

	Phoenix	Standard ^{235}U Core	Cycle 108	20% ^{235}U
No. of fixed fuel elements	19	23	23	23
No. of plates per element	16	19	19	19
No. of fuel-follower shims	8	4	4	4
No. of plates per element	13	14	14	14
No. of beryllium-follower shims	0	3	3	3
Fuel in alloy (wt.% in Al)	21% Pu	18% U	14% Pu	64% U
Fuel thickness	0.040 in.	0.020 in.	0.020 in.	0.030
Clad thickness	0.020 in.	0.015 in.	0.020 in.	0.015
Total fuel in core:				
U	—	5.0 kg	—	23.6 kg
Pu	9.8 kg	—	3.5 kg	—
Isotopics:				
^{235}U	—	93%	—	21.8%
^{238}U	—	7%	—	78.2%
^{238}Pu	0.5%	—	—	—
^{239}Pu	65.3%	—	95.4%	—
^{240}Pu	23.2%	—	4.3%	—
^{241}Pu	7.6%	—	0.3%	—
^{242}Pu	3.4%	—	—	—

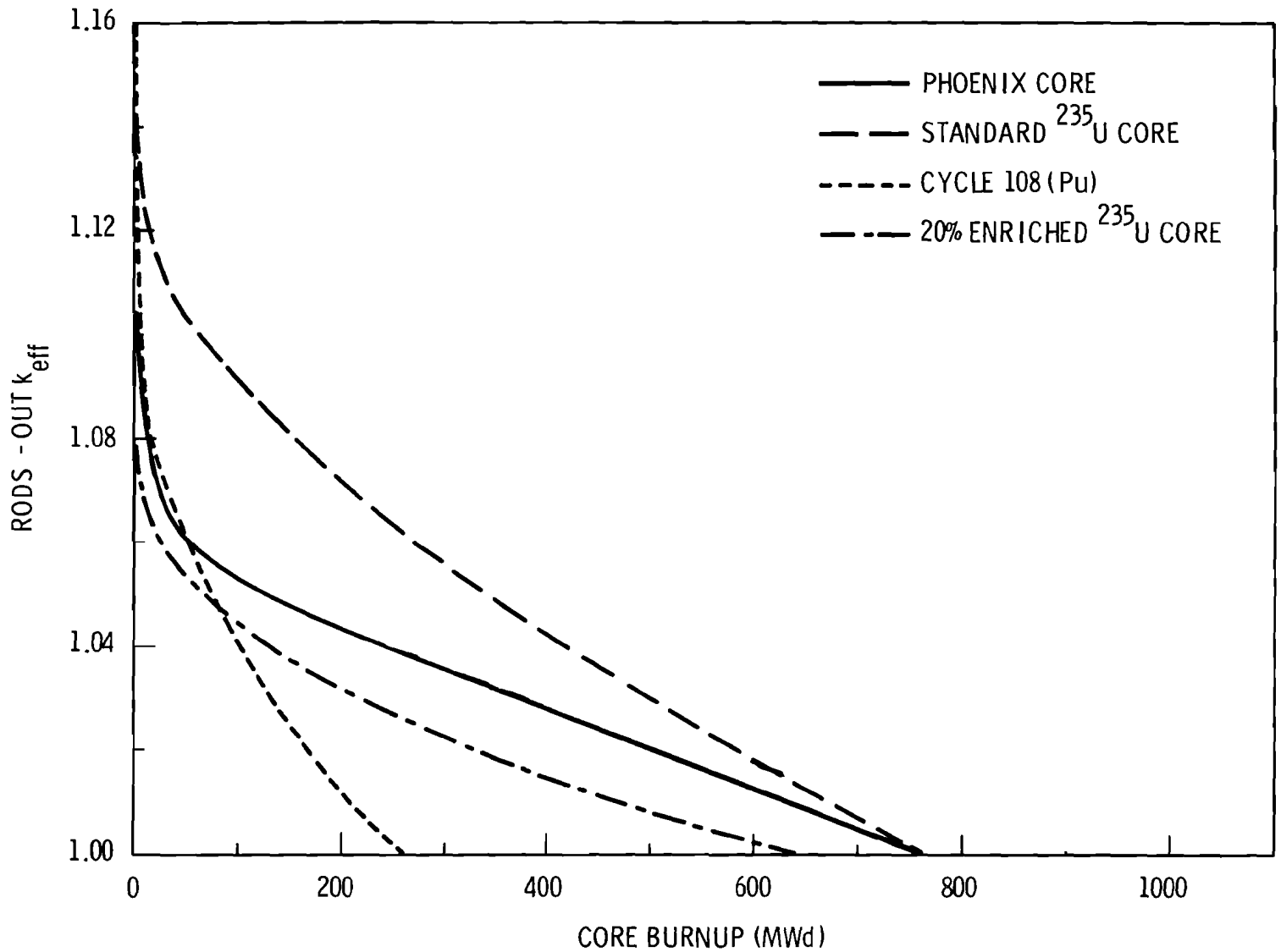

FIGURE 12. Excess Reactivity vs. Burnup for MTR Cores

The parameters of interest for the four cores are summarized in Table X. The Phoenix core and the 20% enriched core were quite similar in most respects. Both cores produced additional fissionable material during the burnup which reduced the reactivity loss rates significantly below the loss rates observed in the fully enriched cores. An important parameter in a test reactor like MTR is the ratio of the peak thermal neutron flux in the reflector to the reactor power level. This quantity was measured in the three earlier cores but only calculated for the Phoenix core. As shown in Table X, the plutonium-fueled cores produce a significantly higher thermal flux in the reflector per watt of reactor power.

2. Calculated Reactivity Loss Rates

As mentioned previously, the principal calculations made for comparison with the MTR-Phoenix experiment were done using the ZODIAC-G system. The significant differences known to exist between the asymptotic or interior region of the core and the core-reflector interface region were neglected in these calculations. The entire core volume was treated as if it were all in the asymptotic region.

The variation of $k_{effective}$ with burnup is shown in Figure 13 for the adjusted ZODIAC-G calculation and for the experimental result. The ZODIAC-G calculation was normalized to the experimentally determined clean, initial value of 1.104. The power density in the calculation was assumed constant, with a total power of 24 MW. In actual practice,

TABLE X

Burnup Parameters of MTR Cores

	Phoenix	Standard ^{235}U Core	Cycle 108	20% ^{235}U Core
Initial k_{eff}	1.104	1.141	1.160	1.079
Estimated Core Lifetime at Constant Power	765 MWd	755 MWd	262 MWd	646 MWd
Burnup Slope	-0.070 mk/MWd	-0.140 mk/MWd	-0.25 mk/MWd	-0.082 mk/MWd
Average Fuel Burnup	122 MWd/kg fissile	162 MWd/kg fissile	83 MWd/kg fissile	126 MWd/kg fissile
Maximum Core Power	24 MW	40 MW	30 MW	30 MW
Peak Thermal Neutron Flux/Watt in Reflector	Not Measured Calculated	$\frac{\sim 3.5 \times 10^{14}}{30 \times 10^{6}}$	$\frac{\sim 7 \times 10^{14}}{30 \times 10^{6}}$	$\frac{\sim 2.5 \times 10^{14}}{30 \times 10^{6}}$
	$\sim 2 \times 10^{7}$	1.16×10^{7}	2.3×10^{7}	0.8×10^{7}

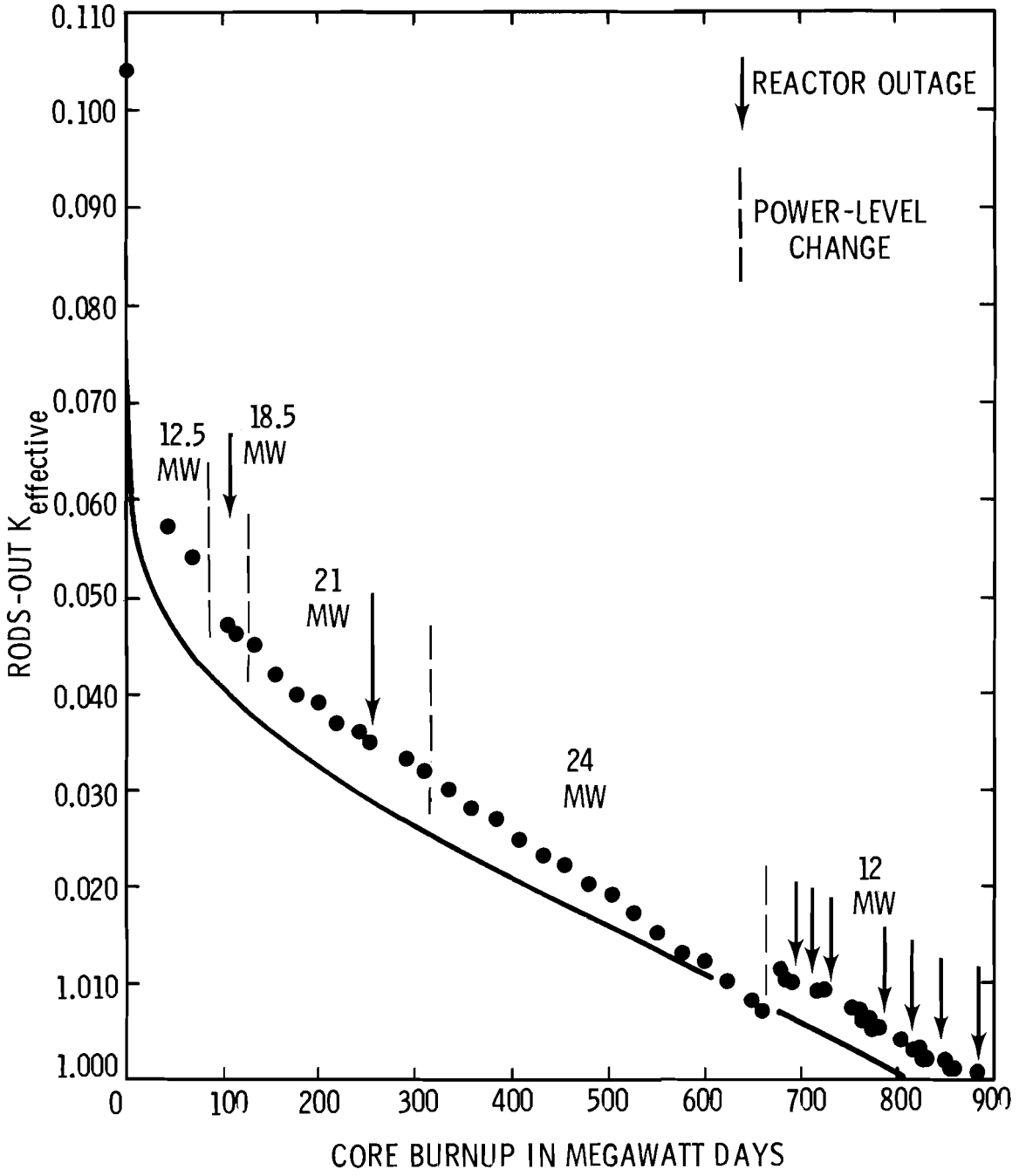

FIGURE 13. Variation of MTR-Phoenix Core Reactivity, Measured and Calculated.

the reactor was operated at power levels of 12.5, 18.5 and 21 MW prior to reaching 24 MW as shown in Figure 4, so there is some question about the equilibrium status of the saturating fission products until well after reaching 24 MW. The only portion of the core burnup that was in reasonable equilibrium status was between about 350 and 650 MWd. Subsequent operations were at 12 MW and for short periods of time, making it unlikely that any of the later measurements of $k_{effective}$ are characteristic of an equilibrium condition. Another complicating factor was introduced as the shim rods were withdrawn during burnup, thus allowing the core power to be produced in a larger volume of the core and reducing the average power density throughout the core. Therefore, it is difficult to make any clearcut comparisons between the calculation and the experiment. It is, however, interesting to compare the slopes of the burnup curves in the 350-650 MWd range. The experimental curve yields a slope of -0.069 milli-k/MWd while the ZODIAC-G calculation yields -0.050 milli-k/MWd, a discrepancy of about 28%.

CONCLUSIONS

It is not obvious from the data or the calculations just where the main problem lies. In all probability, the discrepancies are the accumulative result of a number of difficulties. The measured isotopic data demonstrated the significant differences produced by interactions with the reflector at the core boundary. Since the burnup calculation utilized asymptotic core conditions throughout, this simplification is an obvious suspect. The fission product poison model neglected ^{105}Rh in the treatment of saturating poisons. Depending upon the thermal flux level in the core, ^{105}Rh can be a significant neutron absorber in plutonium-fueled cores. The burnup calculation was performed in one-dimension, rather than in the very complex x,y,z geometry of the actual core. This additional simplification is another likely source of discrepancies.

Despite the differences between experiment and analysis, the MTR-Phoenix fuel program has produced several valuable results.

- The basic premise of the Phoenix concept, that ^{240}Pu could be utilized as a convertible poison to obtain longer reactivity lifetimes without increasing initial reactivity, was demonstrated.
- A significant body of data was created which relates the variation of plutonium isotopic compositions with burnup, in different neutron energy spectra.

These data provide an important and unique base against which further modifications and improvements in calculational models and methods can be tested.

REFERENCES

1. E. C. Davis, Jr., R. I. Smith, and L. D. Williams, Critical Experiments in an MTR Mockup Using Phoenix Fuel, BNWL-1481, Battelle Memorial Institute, Pacific Northwest Laboratories, Richland, Washington, June 1970.

2. D. G. Albertson and G. J. Busselman, "Analysis and Measurement of Pu Al-Polyethylene Systems in the PCTR," Trans. Am. Nuc. Soc., 8, 448 (1965).

3. W. P. Stinson and C. M. Heeb, "Approach-to-Critical Experiments with Phoenix Fuel," Trans. Am. Nuc. Soc., 10, 187 (1967).

4. C. M. Heeb, Analysis of the Phoenix Fuel Experiments, BNWL-1514, Battelle Memorial Institute, Pacific Northwest Laboratories, Richland, Washington, October 1970.

5. J. W. Kutcher and E. C. Davis, The MTR-Phoenix Fuel Experiment: Critical Test and Burnup Results, BNWL-1593, Battelle Memorial Institute, Pacific Northwest Laboratories, Richland, Washington, June 1971.

6. R. J. Nertney et al, Fundamentals in the Operation of Nuclear Test Reactors, Volume 2, Materials Testing Reactor Design and Operation, IDO-16871-2, Phillips Petroleum Company (1963).

7. R. S. Marsden, R. L. Curtis, and D. W. Knight, Safety Analysis Report for the MTR Phoenix Fuel Experiments, IN-1209, Idaho Nuclear Corporation (1969).

8. D. R. Skeen and L. J. Page, THERMOS/BATTELLE: The Battelle Version of the THERMOS Code, BNWL-516, Pacific Northwest Laboratories (1967).

9. D. D. Matsumoto and R. H. Holeman, "ZODIAC G," Plutonium Utilization Program Technical Activities Quarterly Report, December 1967, January, February, 1968, BNWL-739, Pacific Northwest Laboratories (1968).

10. J. L. Carter, Jr., HRG-3: A Code for Calculating the Slowing Down Spectrum in the P1 or B1 Approximation, BNWL-1432, Pacific Northwest Laboratories (1970).

11. J. R. Lilley, Computer Code HFN-Multigroup, Multiregion Neutron Diffusion Theory in One Spece Dimension, HW-71545, Hanford Laboratories (1961).

12. B. H. Duane, "Time Variant Isotopic Transmutation GE-HL Program ALCHEMY," Physics Research Quarterly Report, October, November, December, 1963, HW-80020, Hanford Laboratories (1964).

REFERENCES (Continued)

13. E. A. Nephew, Thermal and Resonance Absorption Cross Sections of the U^{233}, U^{235}, and Pu^{239} Fission Products, ORNL-2869, Oak Ridge National Laboratory, (1960).

14. R. P. Matsen, "A Technique for the Determination of Ratios of Effective Cross Sections from Reactor Fuel Burnup Data," Nucl. Sci. & Eng., 32, 267 (1968).

15. R. P. Matsen, DBUFIT-1, A Least Squares Analysis Code for Nuclear Burnup Data, BNWL-1396, Pacific Northwest Laboratories (1970).

APPENDIX A

ANALYTICAL RESULTS FROM PHOENIX FUEL WAND SAMPLES

Lab. No. W1127
Cus. No. Wand #8, Sample #4.
Date 2-22-71
Hour 1800

Gamma Energy Analysis

CE 144	5.4145E+ 8	0.81%
CE 141	1.0309E+ 7	7.5%
RU 103	3.0278E+ 7	3.8%
RU 106	5.2406E+ 8	1.2%
CS 134	4.8782E+ 6	8.1%
CS 137	5.6622E+ 7	1.8%
ZR 95	1.5375E+ 8	1.4%
NB 95	2.8945E+ 8	0.65%

Lab. No. W1128
Cus. No. Wand #8, Sample #5.
Date 2-22-71
Hour 1830

Gamma Energy Analysis

CE 144	9.0082E+ 8	0.89%
CE 141	1.4589E+ 7	9.7%
RU 103	5.3307E+ 7	3.9%
RU 106	9.7106E+ 8	1.2%
CS 134	1.5843E+ 7	5.5%
CS 137	9.6540E+ 7	1.9%
ZR 95	2.4187E+ 8	1.6%
NB 95	4.2689E+ 8	0.76%

Lab. No. W1129
Cus. No. Wand #8, Sample #6.
Date 2-22-71
Hour 1850

Gamma Energy Analysis

CE 144	1.1598E+ 9	0.76%	(DIS/MIN)/ML
CE 141	1.8651E+ 7	8.1%	(DIS/MIN)/ML
RU 103	4.7577E+ 7	4.7%	(DIS/MIN)/ML
RU 106	9.0151E+ 8	1.3%	(DIS/MIN)/ML
CS 134	2.2810E+ 7	4.3%	(DIS/MIN)/ML
CS 137	1.2326E+ 8	1.7%	(DIS/MIN)/ML
ZR 95	3.0218E+ 8	1.4%	(DIS/MIN)/ML
NB 95	5.3631E+ 8	0.68%	(DIS/MIN)/ML

Lab. No. W1130
Cus. No. Wand #12, Sample #1.
Date 2-22-71
Hour 1950

Gamma Energy Analysis

CE 144	3.2059E+ 8	0.77%
CE 141	4.6569E+ 6	8.2%
RU 103	2.6602E+ 6	22%
RU 106	5.0192E+ 7	5.5%
CS 134	1.3882E+ 6	11%
CS 137	3.4283E+ 7	1.8%
ZR 95	7.9455E+ 7	1.6%
NB 95	1.5299E+ 8	0.72%

Lab. No. W1131
Cus. No. Wand #12, Sample #2.
Date 22-22-71
Hour 2010

Gamma Energy Analysis

CE 144	6.5407E+ 8	0.70%
CE 141	8.6403E+ 6	8.8%
RU 103	1.9950E+ 7	5.6%
RU 106	4.4093E+ 8	1.4%
CS 134	5.6941E+ 6	7.1%
CS 137	6.8958E+ 7	1.6%
ZR 95	1.5824E+ 8	1.4%
NB 95	3.0475E+ 8	0.63%

Lab. No. W1132
Cus. No. Wand #12, Sample #3.
Date 2-22-71
Hour 2040

Gamma Energy Analysis

CE 144	7.7702E+ 8	0.63%	(DIS/MIN)/ML
CE 141	9.4364E+ 6	8.3%	(DIS/MIN)/ML
RU 103	1.4837E+ 7	7.8%	(DIS/MIN)/ML
RU 106	3.3120E+ 8	1.8%	(DIS/MIN)/ML
CS 134	9.7102E+ 6	4.9%	(DIS/MIN)/ML
CS 137	8.3172E+ 7	1.4%	(DIS/MIN)/ML
ZR 95	1.8512E+ 8	1.3%	(DIS/MIN)/ML
NB 95	3.4137E+ 8	0.60%	(DIS/MIN)/ML

Relative 1 σvalue based on theoretical counting statistics only.

Base 10 exponent. i.e. for Nb 95: 1.5299 x 10^8 (± .72% 1 σ) dpm/ml

Note: The ^{137}Cs values, obtained by direct (without chemical separation) gamma spectrometric analysis (GSA) using a high resolution Ge(Li) detector may be converted from the dpm/ml values given on the teletype output sheets to comparable atoms/mℓ values by multiplying by 2.3 x 10^{10}. The GSA values are inherently less reliable than the values from the standard method.

ANALYTICAL RESULTS ON PHOENIX FUEL WAND SAMPLES

Wand Number:	12-SA1	12-SA2	12-SA3	8-SA4	8-SA5	8-SA6	1-SA7
Lab. Number	W1130	W1131	W1132	W1127	W1128	W1129	W1126
Gross Sample Weight(1) g/liter	7.882	8.274	7.388	7.682	7.186	8.144	7.088
Dimensions:							
Pu Sample Vol.(2)	0.10010	0.10010	0.10010	0.10010	0.10010	0.10010	0.10010
Pu Spike Vol.(2)	0.34950	0.34950	0.34950	0.34950	0.34950	0.34950	0.34950
238/239 (Pu Sample)	0.00982 (20)(3)	0.01169 (20)	0.01334 (20)	0.01132 (20)	0.01460 (30)	0.01598 (30)	0.00811 (10)
240/239 " "	0.3925 (12)	0.4361 (13)	0.4678 (14)	0.4223 (13)	0.4969 (15)	0.5142 (16)	0.3488 (10)
241/239 " "	0.1334 (7)	0.1747 (8)	0.2120 (11)	0.1592 (6)	0.2292 (11)	0.2536 (12)	0.0928 (5)
242/239 " "	0.05839 (60)	0.06902 (70)	0.07921 (80)	0.06548 (70)	0.08717 (90)	0.09429 (90)	0.04896 (50)
239/242 (Pu Sample + Spike)(4)	0.7189 (22)	0.6738 (30)	0.5444 (16)	0.6335 (19)	0.4893 (15)	0.5306 (16)	——
Nd Sample Vol.(2)	1.99958	1.49911	0.99814	1.49911	0.99814	0.79966	——
Nd Spike Vol.(2)	0.39969	0.39969	0.39969	0.39969	0.39969	0.39969	——
150/142 (Nd Sample)	43.23 (20)	72.92 (40)	83.89 (40)	64.35 (30)	81.15 (40)	82.34 (40)	——
150/148 " "	0.5889 (20)	0.5762 (20)	0.5720 (20)	0.5850 (20)	0.5761 (20)	0.5768 (20)	——
142/150 (Nd Sample + Spike)(5)	0.00863 (5)	0.00818 (4)	0.00800 (4)	0.00840 (4)	0.00806 (5)	0.00799 (4)	——
148/150 " " " "	0.1357 (4)	0.1906 (6)	0.1586 (5)	0.1598 (5)	0.1752 (5)	0.1825 (6)	——
^{137}Cs (atoms/ml)(6)	$8.495 \times 10^{17} \pm 0.55\%$	$1.647 \times 10^{18} \pm 0.19\%$	$1.970 \times 10^{18} \pm 0.19\%$	$1.364 \times 10^{18} \pm 0.11\%$	$2.269 \times 10^{18} \pm 0.74\%$	$2.912 \times 10^{18} \pm 0.51\%$	——
^{133}Cs Wt% (Cs)(7)	Not Analyzed	Not Analyzed	47.3	Not Analyzed	Not Analyzed	45.9	Insufficient Cesium to analyze
^{134}Cs " "			0.35			0.58	
^{135}Cs " "			6.9			8.5	
^{137}Cs " "			45.45			45.02	

Note:

(1) Based on gross weight of PuAl alloy core plus 40 mil thick aluminum cladding dissolved and diluted to 50 milliliters. Actual weights of sample sections analyzed were .05 times the g/l values.

(2) Sample and spike volumes are in milliliters.

(3) Numbers in parenthesis following ratios are estimated standard deviations and should be read as follows: 0.01452 (50) = 0.01452 ± 0.00050.

(4) Pu^{242} Spike (ID-8) Volume in ml, Calib: 4.9805×10^{16} atoms ^{242}Pu/ml, Ratio: 239/242 = .000103.

(5) Nd^{150} Spike (ID-14), Calib: 7.84×10^{15} atoms ^{150}Nd/ml, Isotopic Ratios: $\frac{142/150}{.008056}$ $\frac{148/150}{.008679}$

(6) Our standard method of analysis for Cs-137 for burnup determinations was used. (Cesium separation by tetraphenyl borate solvent extraction followed by direct gamma spectrometric--NaI (Tl) scintillation well crystal--comparison to the Nuclear Chicago/ASTM cesium-137 standard calibrated by mass spectrometry in terms of atoms of Cs^{137}.) 30.12 years was the half life value used to correct for radioactive decay of the Cs-137 standard since 8/8/62. Date counted: 2/22/71.

(7) Cesium isotopics measured on 3/15/71 and 3/12/71 for samples W1132 and W1129, respectively.

APPENDIX B

ANALYTICAL RESULTS FROM PHOENIX FUEL PLATE SAMPLES

ANALYTICAL RESULTS ON PHOENIX FUEL PLATE SAMPLES

Plate Number:	22-8 #1	3-8 #2
Lab. Number:	W1429	W1430
Gross Sample Weight[1]	0.7628 g/100 mℓ	0.9572 g/100 mℓ
Dimensions:	0.427"[2] x 0.473"	0.492"[2] x 0.506"
Pu Sample Vol.[3]	0.009512	0.009512
Pu Spike Vol.[3]	0.34950	0.39969
238/239 (Pu Sample)	0.01452 (50)[4]	0.01688 (50)[4]
240/239 " "	0.4923 (15)	0.6045 (20)
241/239 " "	0.1824 (9)	0.2048 (10)
242/239 " "	0.07551 (80)	0.09870 (90)
239/242 (Pu Sample + Spike)[5]	0.6764 (20)	0.4267 (10)
Nd Sample Vol.[3]	0.04746	0.02376
Nd Spike Vol.[3]	0.34950	0.34950
150/142 (Nd Sample)	74.22 (1.50)[4]	48.38 (80)[4]
150/148 " "	0.5826 (30)	0.5737 (30)
142/150 (Nd Sample + Spike)[6]	0.00744 (10)	0.00765 (10)
148/150 " " " "	0.1082 (5)	0.0728 (4)
^{137}Cs (atoms/mℓ)[7]	2.43×10^{16} (on 4/30/71)	3.00×10^{16} (on 4/30/71)
^{133}Cs Wt% (Cs)[8]	47.24 ± 0.4	49.01 ± 0.4
^{134}Cs " "	0.564 ± 0.006	0.601 ± 0.006
^{135}Cs " "	11.04 ± 0.1	7.44 ± 0.07
^{137}Cs " "	41.15 ± 0.4	42.94 ± 0.4

NOTE:

(1) Gross sample weight of 40 mil thick Pu-Al "meat" plus 20 mil Al cladding on each side dissolved and made up to 100 mℓ total volumes. Surface contamination was removed as effectively as possible by wiping the surfaces of the pieces with cotton swabs moistened with ethanol before weighing and dissolution.

(2) Both plates had a saw "burr" in the same position. This measurement is an average.

(3) Sample and Spike Volumes are in milliliters.

(4) Numbers in parenthesis following ratios are estimated standard deviations and should be read as follows: 0.01452 (50) = 0.01425 ± 0.00050.

(5) Pu^{242} spike (ID-8) Volume in mℓ. Calib. 4.9805×10^{16} atoms ^{242}Pu/mℓ

Ratio: 239/242 = 0.000103

(6) Nd^{150} Spike (ID-14), Calib. 7.84 x 10^{15} atoms ^{150}Nd/mℓ

Ratios: 142/150 = 0.008056 148/150 = 0.008679

(7) The ^{137}Cs values from direct gamma spectrometric analysis (GSA) may be converted from dpm/mℓ values given on the teletype output to comparable atoms/mℓ values by multiplying by 2.3 x 10^7. The GSA results are inherently less reliable than these obtained from our standard "burnup" method.

(8) Some problems were encountered with getting the original aliquots taken for Cs to "run" on the mass spectrometer. An undetermined fraction of the ^{133}Cs observed could be from natural contamination rather than fission product origin. The absence of a "blank" sample for comparison precludes accurate estimation of the amount of natural Cs contamination.

LAB.NO. W143Ø
CUS.No. 3-8
DATE 5/6/71
HOUR 135Ø

GAMMA ENERGY ANALYSIS

CE 144		1.Ø155E+1Ø	2.2%	(DIS/MIN)/ML
CE 141	<	4.8259E+ 7		(DIS/MIN)/ML
RU 1Ø3		2.2969E+ 8	24%	(DIS/MIN)/ML
RU 1Ø6		1.234ØE+1Ø	3.1%	(DIS/MIN)/ML
CS 134		2.5222E+ 8	13%	(DIS/MIN)/ML
CS 137		1.2529E+ 9	5.Ø%	(DIS/MIN)/ML
ZR 95		1.5372E+ 9	6.6%	(DIS/MIN)/ML
NB 95		4.Ø194E+ 9	2.4%	(DIS/MIN)/ML

LAB.NO. W1429
CUS.NO. 22-8
DATE 5/6/71
HOUR 1325

GAMMA ENERGY ANALYSIS

CE 144		8.Ø2Ø8E+ 9	2.5%	(DIS/MIN)/ML
CE 141	<	2.965ØE+ 7		(DIS/MIN)/ML
RU 1Ø3		1.6711E+ 8	29%	(DIS/MIN)/ML
RU 1Ø6		9.7975E+ 9	3.4%	(DIS/MIN)/ML
CS 134		1.9113E+ 8	16%	(DIS/MIN)/ML
CS 137		9.7528E+ 8	5.7%	(DIS/MIN)/ML
ZR 95		1.1Ø45E+ 9	8.1%	(DIS/MIN)/ML
NB 95		2.9689E+ 9	2.8%	(DIS/MIN)/ML

Relative 1 σ value based on theoretical counting statistics only

Base 10 exponent, i.e., for Nb-95: 2.9689 x 10^9 (±2.8% 1σ) dpm/mℓ

LAB. NO. W168Ø
CUS. NO. 3-8 #4
DATE 6-22-71
HOUR 1345

GAMMA ENERGY ANALYSES

CE 144		5.Ø454E+	9	Ø82%	(DIS/MIN)/ML
CE 141	<	4.636ØE+	6		(DIS/MIN)/ML
RU 1Ø3		4.8ØØ5E+	7	17%	(DIS/MIN)/ML
RU 1Ø6		6.3Ø35E+	9	1.0%	(DIS/MIN)/ML
CS 134		1.1871E+	8	5.4%	(DIS/MIN)/ML
CS 137		6.7813E+	8	1.7%	(DIS/MIN)/ML
ZR 95		4.885ØE+	8	3.2%	(DIS/MIN)/ML
NB 95		8.6331E+	8	1.4%	(DIS/MIN)/ML

LAB.NO. W1679
CUS.NO. 22-8 #3
DATE 6-22-71
HOUR 132Ø

GAMMA ENERGY ANALYSIS

CE 144	4.4429E+	9	Ø88%	(DIS/MIN)/ML
CE 141	1.1542E+	7	48%	(DIS/MIN)/ML
RU 1Ø3	4.141ØE+	7	19%	(DIS/MIN)/ML
RU 1Ø6	5.4913E+	9	1.1%	(DIS/MIN)/ML
CS 134	1.Ø432E+	8	5.8%	(DIS/MIN)/ML
CS 137	6.ØØ97E+	8	1.8%	(DIS/MIN)/ML
ZR 95	4.3335E+	8	3.4%	(DIS/MIN)/ML
NB 95	7.49Ø1E+	8	1.5%	(DIS/MIN)/ML

Relative 1σ value based on theoretical counting statistics only

Base 10 exponent, i.e., for Nb-95: 7.4901 x 10^9 (±1.5% 1σ) dpm/mℓ

BNWL-1756
Special Distribution
in Category UC-80

No. of
Copies

OFFSITE

1 AEC Chicago Patent Group

G. H. Lee

7 AEC Division of Reactor Development and Technology

Director, RDT
Asst. Dir., Project Management
Chief, Water Projects Branch (2)
Asst. Dir., Reactor Technology
Chief, Reactor Physics Branch (2)

3 AEC Technical Information Center

3 Argonne National Laboratory

R. Avery
C. H. Bean
R. E. Machery

1 Atomic Energy of Canada Limited

Chalk River Nuclear Laboratory
Reactor Physics Branch
Chalk River, Ontario, Canada

M. Duret

1 Babcock and Wilcox

P.O. Box 1260
Lynchburg, VA 24505

H. M. Jones

1 Bhabha Atomic Research Centre

Theoretical Physics Section/RED
Central Complex Bldg.
Trombay, Bombay-85, India

S. R. Dwivedi

No. of Copies	
1	Brookhaven National Laboratory G. Price
3	Combustion Engineering P. O. Box 500 Windsor, Connecticut 06095 R. Harding R. Hellens S. Visner
1	Commonwealth Edison Company 72 West Adams Street Chicago, Ill. A. Veras
1	Consumers Power Company 1945 W. Parnall Road Jackson, Mich. 49201 G. J. Walke
2	CNEN - Centro Studi-Nuclearie Casaccia, Rome, Italy Ugo Farinelli Paolo Loizzo
1	EBASCO Services 2 Rector St. New York, N. Y. 10006 D. deBoisblanc
2	Edison Electric Institute 750 Third Avenue New York, N. Y. 10017 John J. Kearney George Watkins

No. of Copies	
2	E. I. du Pont deNemours & Company, Inc., SRL G. Dessauer H. Honeck
1	ENEL Via G. B. Martini (Pizaaz Verdi) Rome, Italy Mr. Paloetti Gaulandi
2	General Electric Co., San Jose Nuc. Dev. and Eng. 175 Curtner Avenue San Jose, California 95112 D. L. Fischer R. L. Crowther
2	General Electric Co., Vallecitos Atomic Lab. P. O. Box 846 Pleasanton, California 94566 D. G. Albertson T. M. Snyder
7	Idaho Nuclear Corporation R. M. Brugger E. E. Burdick N. C. Kaufman (5)
1	Japan Atomic Energy Institute TCA-JPDR Tokai-Mura, Naka-Gun, Ibaraki-Ken Japan Shojiro Matsuura

No. of Copies	
1	Massachusetts Institute of Technology 1338 Albany Street Bldg. NW 12 Cambridge, Mass. 02139 D. D. Lanning
1	Nuclear Materials and Equipment Corp. Penn Center Apollo, Penn. 15613
1	NUKEM D-645, HANAU POSTFACH 869 Germany Mr. Wolgang K. L. Jager
1	Philadelphia Electric Company 1000 Chestnut Street Philadelphia 5, Pa. Mr. Wayne C. Astley
1	Power Reactor & Nuclear Fuel Development Corp. 9-13, 1- chome, Akaska Minato-ku, Tokyo, Japan Setsuo Kobayashi
1	S. C. K. - C. E. N. MOK-DONK Belgium Dr. H. Vanden Broeck BRL.
1	United Nuclear Corporation Research & Engineering Center Grasslands Road Elmsford, New York 10523 J. R. Tomonto

No. of Copies	
4	Westinghouse Electric Corporation Atomic Power Division Post Office Box 355 Pittsburgh, Penn. 15230 R. J. French R. S. Miller W. L. Orr J. R. Worden

ONSITE

1	AEC/RL Patent Attorney R. M. Poteat
1	AEC/RL - Sr. Site Representative, PNP F. Standerfer
1	AEC Richland Operations Office B. J. Melton
5	United Nuclear Industries C. D. Harrington N. R. Miller UNI Files (3)
6	Hanford Engineering Development Laboratory R. A. Bennett E. N. Heck P. L. Hofmann HEDL Document Control (3)

No. of Copies	
45	Battelle-Northwest

E. L. Alpen
S. H. Bush
J. L. Carter
N. E. Carter
D. E. Christensen
D. L. Condotta
D. E. Deonigi
J. C. Fox
M. D. Freshley
S. Goldsmith
C. M. Heeb
H. L. Henry
U. P. Jenquin
B. M. Johnson
G. J. Konzek
D. A. Kottwitz
B. R. Leonard, Jr.
R. C. Liikala
D. F. Newman
D. R. Oden
H. M. Parker
L. T. Pedersen
W. W. Porath
D. L. Prezbindowski
W. L. Purcell
W. D. Richmond
G. D. Seybold
L. C. Schmid
R. I. Smith (5)
D. H. Thomsen
V. O. Uotinen
L. D. Williams
W. C. Wolkenhauer
M. G. Zimmerman
Technical Information (5)
Technical Publications (2)